Controlling swarms towards flocks and mills

José A Carrillo, Dante Kalise, Francesco Rossi, Emmanuel Trélat

Controlling swarms towards flocks and mills

José A. Carrillo* Dante Kalise† Francesco Rossi‡ Emmanuel Trélat§

Abstract

Self-organization and control around flocks and mills is studied for second-order swarming systems involving self-propulsion and potential terms. It is shown that through the action of constrained control, is it possible to control any initial configuration to a flock or a mill. The proof builds on an appropriate combination of several arguments: LaSalle invariance principle and Lyapunov-like decreasing functionals, control linearization techniques, and quasi-static deformations. A stability analysis of the second-order system guides the design of feedback laws for the stabilization to flock and mills, which are also assessed computationally.

1 Introduction

We analyse the controllability of the interacting particle system of N agents on the plane, governed by second-order dynamics

$$\begin{aligned} \dot{x}_i(t) &= v_i(t) \\ \dot{v}_i(t) &= (\alpha - \beta|v_i(t)|^2)v_i(t) - \frac{1}{N}\sum_{\substack{j=1 \\ j\neq i}}^{N} \nabla W(x_i(t) - x_j(t)) + u_i(t)\,, \end{aligned} \tag{1}$$

where $x_i(t) \in \mathbb{R}^2$ (resp., $v_i(t) \in \mathbb{R}^2$) is the position (resp., the velocity) of the i^{th} agent. In this model, the term $(\alpha - \beta|v_i|^2)v_i$, where $\alpha \geqslant 0$ and $\beta > 0$ are fixed, represents a *self-propulsion* force, while

$$F_i(x) = \frac{1}{N}\sum_{\substack{j=1 \\ j\neq i}}^{N} \nabla W(x_i - x_j), \qquad F = (F_1, \dots, F_N)^\top\,, \tag{2}$$

expresses a *attraction-repulsion* force through the pairwise interaction potential W. The control $u = (u_1, \dots, u_N)$, with $u_i(t) \in \mathbb{R}^2$, is subject to the constraint $\|u(t)\| \leqslant M$ for almost every $t \in \mathbb{R}$, where $M > 0$ is fixed. Here, $|\cdot|$ is the Euclidean norm in $\mathbb{R}^2$ and $\|\cdot\|$ is the ∞-norm in $(\mathbb{R}^2)^N$ or $(\mathbb{R}^2)^{2N}$ associated to $|\cdot|$, i.e.,

$$\|v\| = \max_{i=1,\dots N} |v_i|, \qquad \|(x,v)\| = \max_{i=1,\dots N} |x_i| + \max_{i=1,\dots N} |v_i|.$$

*Mathematical Institute, University of Oxford, Oxford OX2 6GG, UK (carrillo@maths.ox.ac.uk).

†School of Mathematical Sciences, University of Nottingham, UK (dante.kalise@nottingham.ac.uk).

‡Dipartimento di Matematica "Tullio Levi-Civita", Università degli Studi di Padova, Via Trieste 63, 35121 Padova, Italy (francesco.rossi@math.unipd.it).

§Sorbonne Université, CNRS, Université de Paris, Inria, Laboratoire Jacques-Louis Lions (LJLL), F-75005 Paris, France (emmanuel.trelat@sorbonne-universite.fr).

Models of the form (1) are particular examples of agent-based models (ABMs). ABMs appear in biology, mathematics, physics, and engineering in order to describe the motion of a collection of N individual entities at the microscopic scale interacting through simple rules. These types of models have been proposed to describe the flocking of birds [16, 48, 50], the schooling of fish [7, 11, 13, 37, 39], and swarms of bacteria [43], among others. We refer to the surveys [24, 44] for more general models in the area of interacting particle systems in collective behavior.

The model (1) was introduced in [47] and extensively studied in [12, 29, 34] giving a detailed description of patterns and stability properties of particular solutions through numerical experiments. The role of the self-propulsion term of strength $\alpha > 0$ versus friction of strength $\beta > 0$ is to fix a typical cruise speed for agents. In fact, in the absence of interactions $W = 0$ (no potential) and $u = 0$ (no control) in (1), except for the unstable equilibrium $v = 0$, all trajectories converge to $|v_i|^2 = \frac{\alpha}{\beta}$ along heteroclinic orbits. These terms will actually promote the appearance of particular solutions : *flock* and *mill* solutions (defined below). Even more complicated solutions as double-mills have been studied in the literature [22].

We assume throughout the article that the interaction potential is radial $W(x) = U(|x|)$, with U of class C^2 except possibly at the origin, and that the interactions are negligible for large distances $\lim_{r\to+\infty} U'(r) = 0$. Typical potentials used in previous works are Morse potentials of the form $U(r) = -C_A e^{-r/\ell_A} + C_R e^{-r/\ell_R}$, the index A standing for "attractive" and the index R for "repulsive". As shown in [12, 34], the interesting region is when $\ell = \frac{\ell_R}{\ell_A} < 1$ and $C = \frac{C_R}{C_A} > 1$. In this case, the derivative U' of the potential is such that $|U'|$ is bounded, U' is positive up to some $r_0 > 0$, and is then negative and converging to 0 as $r \to +\infty$. We will refer to this kind of potentials as bounded repulsive-attractive potentials. Other potentials of interest are power-law potentials [45, 10] given by $U(r) = \frac{|r|^a}{a} - \frac{|r|^b}{b}$ with $b < a < 0$, for which we have $U'(0) = -\infty$, thus avoiding collisions due to an increasing repulsion whenever two particles get closer. We will refer to this kind of potentials as unbounded repulsive-attractive potentials.

Another family of ABMs of interest arises when introducing alignment mechanisms in the modeling. A basic example of this family is the Cucker-Smale model introduced in [32, 33] and further developed in [23, 35, 36, 49], among others. The main phenomenon in those models is the emergence of alignment, i.e. consensus in velocity. Imposing consensus in velocity has also been analysed from the point of view of control [14, 17, 18, 38]. These consensus models also have applications in swarm robotics [27, 28], social and pedestrian dynamics [3, 2, 42, 59] where control theory is applied with different regulation objectives expressed in both ad-hoc and optimal control designs [4, 5, 8, 15].

Despite the simplicity of the model (1), a striking phenomenon regarding the long-time asymptotics of solutions occurs. There are several stable self-organized patterns that emerge from these dynamics depending on the initial data even for the same parameter values and interaction potentials [29, 34]. More precisely, flock and mill solutions, which are relevant examples of self-organized configurations for the swarming model, appear asymptotically. Flock and mill solutions are not equilibria in the classical sense (with $\dot{x}_i = \dot{v}_i = 0$ for all $i = 1, \dots, N$), but are rather solutions with specific invariance properties inherited from (1). Flock solutions describe configurations with agents moving by uniform translation: a *flock* is a trajectory $(x(t), v(t)) = (x^* + tv^*, v^*)$ in which the velocities $v^* = (v_1^*, \dots, v_N^*)$ are identical and satisfy $|v_i^*| = \sqrt{\frac{\alpha}{\beta}}$. A *flock ring* is a flock in which the position of agents x_i are equally distributed on a circle with a certain radius R, i.e.,

$$\hat{x} = (\hat{x}_1, \dots, \hat{x}_N) \in \mathbb{R}^{2N}, \quad \hat{x}_i = R\,\mathcal{R}_\theta^i \begin{pmatrix} \cos\left(\frac{2\pi}{N}\right) \\ \sin\left(\frac{2\pi}{N}\right) \end{pmatrix}, \quad \mathcal{R}_\theta = \begin{pmatrix} \cos(\theta) & -\sin(\theta) \\ \sin(\theta) & \cos(\theta) \end{pmatrix}.$$

A *mill* for (1) corresponds to N agents rotating with a constant angular velocity ω with respect to a center c, i.e., $(x_i(t), v_i(t)) = (\mathcal{R}_{\omega t}(x_i^* - c) + c, \mathcal{R}_{\omega t} v^*)$ for some $(x^*, v^*) \in \mathbb{R}^{4N}$. A *mill ring* is

a mill in which the position of agents x_i are moreover equally distributed on a circle with a certain radius R, i.e., $x^* = \hat{x}$. As a consequence, velocities satisfy

$$v_i^* = \frac{1}{R}\sqrt{\frac{\alpha}{\beta}}\,\hat{x}_i^\perp \qquad \text{with} \qquad \hat{x}_i^\perp = \mathcal{R}_{\pi/2}\hat{x}_i.$$

The particular case of flock and mill rings has been studied in detail in terms of linear stability properties [12, 45]. Notice that the spatial profiles of flock solutions to (1) correspond to stationary states of the first order model

$$\dot{x}_i = -\sum_{\substack{j=1\\ j\neq i}}^{N} \nabla W\left(x_j - x_i\right), \quad i = 1, \dots, N. \tag{3}$$

The stability analysis of general linear and nonlinear flocks and mills has been fully studied in [1, 26]. Flock shapes, stationary states for (3), for different potentials can have many different shapes even for biologically motivated potentials [45, 12, 58, 25], and their regularity heavily depends on the repulsion strength at the origin, see [10, 9, 21]. Characterizing all possible mill and flock profiles for a given potential is equivalent to characterizing all possible stationary states of the first order system (3) or related equations. This difficult problem has not been solved except in very particular choices of the parameters for the power-law potentials. It can be shown that for a repulsive-attractive potential there is a unique flock and mill ring solution and that the radius is characterized uniquely by balances of the relevant forces: attraction, repulsion and centrifugal forces [10, 1]. However, showing that they are the unique flock or mill solution is a challenging problem. It is possible to find potentials for which stable mills exist and they are not rings by numerical experiments. Moreover, some compactly supported potentials generically allow the existence of *flock and mill clusters*, i.e., clusters of particles in which each cluster is a mill, or different flocks in separate directions. For the specific case of flock and mill rings, the radius R is characterized by being a solution to

$$\sum_{p=1}^{N-1} \sin\left(\frac{p\pi}{N}\right) \tilde{U}'\left(2R\sin\left(\frac{p\pi}{N}\right)\right) = 0\,, \tag{4}$$

where $\tilde{U}(r) = U(r) - \omega^2\frac{r^2}{2}$, see [12, 1, 26]. Flock solutions correspond to $\omega = 0$.

Our main goal in this work is to show that constructive controls can be designed to steer the system from any initial data to these various self-organized configurations in interacting particle systems of collective behavior. The main strategy is to prove that the system (1) enjoys interesting controllability properties, such as being able to: steer the system from any initial condition to some/any flock and/or mill; keep the system close to a flock or a mill with an appropriate feedback law; pass from a flock to a mill or conversely. The control u is assumed to satisfy the constraint $\|u\| \leqslant M$ with the minimal threshold $M > 0$ being clearly identified.

The rest of the paper is structured as follows. Section 2 explains in details the main results and the main novelty of our approach: mixing different control techniques wth a deep understanding of the heteroclinic connections in these models. In Section 3, we recall some known stability properties of flocks and mills, together with proposing different feedback designs for transitioning to flock and mill configurations. The control design is guided by controllability results, local stability properties and heteroclinic connections, and is enriched by the use of numerical optimal controls. In Sections 4 and 5, we provide a complete and detailed proof of Theorems 1 and 2.

2 Main results

Our two main results, Theorem 1 in Section 2.1, and Theorem 2 in Section 2.2, deal with bounded and unbounded interaction potentials (as defined in the introduction), respectively. For each statement, we present a brief sketch of our control strategies with a full proof in the last sections.

2.1 First main result: bounded interactions

In our first main result for bounded repulsive-attractive potentials, we assume that our potential is radial, of class C^2, with bounded interactions, i.e., $\sup_{r\geqslant 0} U'(r) < +\infty$ and negligible interactions at ∞, i.e., $\lim_{r\to+\infty} U'(r) = 0$. Since the potential is C^2 at the origin and radial then $U'(0) = 0$. This ensures classical well-posedness of (1) (see Remark 1 further).

Theorem 1. *[Control for bounded interactions] Let $U : [0, +\infty) \to \mathbb{R}$ such that $W(x) = U(|x|)$ is of class C^2 satisfying $U'(0) = 0$, $\lim_{r\to+\infty} U'(r) = 0$ and:*

($\mathbf{U_1}$) *C^2-boundedness: there exist a positive constant C such that $|U(r)| + |U'(r)| + |U''(r)| < C$ for every $r \in [0, +\infty)$.*

If the upper bound M for the control action is such that

$$M > M_{\alpha,\beta} = \sqrt{\frac{4\alpha^3}{27\beta}} \tag{5}$$

then, given any $\bar{v} \in \mathbb{R}^2$ such that $|\bar{v}| = \sqrt{\frac{\alpha}{\beta}}$, the control system can be steered, in sufficiently large time and with a feedback control, from any initial condition to any neighborhood of the flock $(\bar{x}_1 + t\bar{v}, \bar{v}), (\bar{x}_2 + t\bar{v}, \bar{v}), \dots, (\bar{x}_N + t\bar{v}, \bar{v})$ with a control satisfying $\|u\| \leqslant M$.
Denoting by $M_F = \sup_{r>0} |U'(r)|$. Under the stronger assumption

$$M > \max\left(M_{\alpha,\beta},\ M_F\right), \tag{6}$$

the control system can be steered, in sufficiently large time and with a feedback control, from any initial condition to any neighborhood of any flock, flock ring, mill, mill ring.

Remark 1. The result can be generalized to potentials satisfying $U'(0) < 0$, i.e., repulsive at 0 but nonsmooth at 0: for instance, in the case of the widely used Morse potentials [34] in the biologically reasonable, one has bounded interactions up to 0 even if the potential is not C^2 at the origin. In Theorem 1 above, we have assumed that $U'(0) = 0$ to ensure well-posedness and thus avoid technicalities. In the more general case where $U'(0) < 0$, collisions may occur in finite time and thus well-posedness is not a priori ensured; anyway, it is always possible to slightly modify our feedback controls in order to avoid collisions, and thus avoid problematic points for local well-posedness, so essentially we can always assume without loss of generality that the potential is C^2 at the origin if it has bounded interactions.

Remark 2 (The role of the assumptions)**.** The condition (5) means that the control can counteract the natural tendency of the system to stabilize $|v|$ to $\sqrt{\frac{\alpha}{\beta}}$. The value $M_{\alpha,\beta}$ corresponds to the maximum of the function $s \to \alpha s - \beta s^3$ on the half line $s \geqslant 0$, which is attained at $v = \sqrt{\frac{\alpha}{3\beta}}$. Under the condition (6), one can moreover counteract the potential interactions, which allows us to design controls steering the system to any mill. Actually, when the potential allows the existence of cluster mills, it is even possible to steer the system to any such cluster mill configuration.

The control strategy to achieve these various objectives can be made explicit and we will provide it in a *feedback* form, making it particularly convenient to implement in practice. It can even be provided in a *componentwise sparse feedback* form, provided that M is large enough. Hereafter, we explain the controllability strategy, by sketching the proof of Theorem 1 (full detail of the proof is given in Section 4). Given any $\varepsilon > 0$, we set

$$\Omega_\varepsilon = \{(x, v) \in \mathbb{R}^{4N} \ \mid \ v = 0, \ \|F(x)\| \leqslant \varepsilon\}.$$

When $u = 0$, the set Ω_0 (for $\varepsilon = 0$) is invariant under the dynamics. The x-components of each point of Ω_0 are indeed the flocks of the uncontrolled system. Note that, for $\varepsilon > 0$ small, Ω_ε consists both of topological neighborhoods of Ω_0 in the x-variable and of some components "at infinity", where F is small because $\lim_{r\to+\infty} U'(r) = 0$.

Step 1: reaching Ω_ε. The first step of our strategy consists of steering the system from its given (arbitrary) initial condition to the set Ω_ε. To do that, we use the Jurdjevic-Quinn method [40], which is a very powerful approach in control design to derive feedback controls which moreover enjoy instantaneous optimality properties (see [17, 18] as well as [19, 20] for its application to Cucker-Smale multi-agent models). This is done by differentiating with respect to time an appropriate Lyapunov-type functional, then choosing adequately the feedback control, and finally using arguments close to the LaSalle invariance principle.

Step 1.1: Jurdjevic-Quinn stabilization. Defining the Lyapunov functional

$$V = \frac{1}{2}\sum_{i=1}^{N} |v_i|^2 + \frac{1}{2N}\sum_{\substack{i,j=1\\ i\neq j}}^{N} W(x_i - x_j),$$

along the trajectories we have

$$\dot{V} = \sum_{i=1}^{N} (\alpha - \beta|v_i|^2)|v_i|^2 + \langle v_i, u_i\rangle \,,$$

which leads us to define appropriate feedback controls u_i making V decrease: roughly speaking, we would like to take $u_i = -M\frac{v_i}{|v_i|}$ when $|v_i| \leqslant \sqrt{\frac{\alpha}{\beta}}$ and 0 otherwise. Then, using arguments similar to those used in the LaSalle invariance principle, we obtain convergence to Ω_ε. Although this gives the main idea, the complete argument in Section 4.1 is not so easy. The main difficulty is that V is not proper (i.e., V is not infinite at infinity), even taking the quotient with respect to translations. This does not ensure that the system asymptotically reaches a neighborhood Ω_0 as in the classical LaSalle principle, as it can also converge to a component at infinity.

Step 1.2: Reaching Ω_ε in finite time. Once (x, v) is sufficiently close to Ω_ε at time T, both velocities and forces are small. We then apply the control

$$u_i = -(\alpha - \beta|v_i|^2)v_i + F_i(x) - \eta\frac{v_i}{|v_i|}$$

with $\eta > 0$ small to steer each component of $v(T)$ such that $v_i\left(T + \frac{|v_i(T)|}{\eta}\right) = 0$. Note that $|u_i|$ remains small because we are near Ω_ε. By applying this control to each agent, we reach Ω_ε in finite time.

Step 2: Local controllability near Ω_ε. At the end of Step 1, the system is in Ω_ε. Since $v = 0$ and $F(x) \simeq 0$ there, we can set

$$u_i = -(\alpha - \beta|v_i|^2)v_i + F_i(x) + w_i \tag{7}$$

and consider w as a new control, subject to the constraint $\|w\| \leqslant M/2$, and thus focus on the very simple control system

$$\dot{x}_i = v_i, \qquad \dot{v}_i = w_i, \tag{8}$$

near $v = 0$. It is obvious to generate feedback controls w, satisfying $\|w\| \leqslant M/2$, steering this simplified control system from any point in Ω_ε to any other point in a local neighborhood. Note that $\|u\| \leqslant M$, since the agents remain near Ω_ε. Notice that we cannot assure at this stage that two disconnnected components of Ω_ε can be joined by controls of this form, since the size of the control M is disconnected from the size of the force, due to the interaction potential U. In order to choose particular spatial configurations such as flocks or mill rings we control the interaction potential in the next steps by increasing the value for the constraint $\|u\| \leqslant M$ to $M > M_F$.

Step 3: reaching flocks and mills.

Step 3.1: Reaching flocks. Here, we are still under the assumption $M > M_{\alpha,\beta}$. It follows from Step 2 that we can steer the control system to a point near Ω_ε which is such that $F_i(x) \simeq 0$ and $v_i = \nu\bar{v}$ for every $i \in \{1, \dots, N\}$ for some $\bar{v}$ (that we can choose arbitrarily) such that $|\bar{v}| = \sqrt{\frac{\alpha}{\beta}}$ and some $\nu > 0$ small. In other words, we preliminary place the system in a configuration in which all components v_i are small and equal. Note that, in this preliminary step, we are not free to choose the spatial components x_i where we want such as a predetermined flock profile. This will be done in Step 3.3 below, once we assume the size of our control M may overcome the total maximal interaction force.

After having set $v_i = v\bar{v}$, we keep the control active but small to counteract interaction forces ($u_i = F_i \simeq 0$) and we let the system evolve. We have $v_i(t) = v_j(t)$ for all i, j and thus $x_i(t) - x_j(t)$ remains constant. Each variable v_i evolves according to $\dot{v}_i = (\alpha - \beta|v_i|^2)v_i$, starting at the initial value $\nu\bar{v}$, and hence $v_i(t) \to \bar{v}$ as $t \to +\infty$. This is a motion along an heteroclinic orbit, see Section 4.3.

Note that, along this trajectory, in case of unstability the motion can be stabilized by using a feedback control: one linearizes the system along the nominal trajectory, and then correct errors by feedback.

Step 3.2: Passing from a flock velocity to another flock velocity. We now have the control system in a flock and we may want to steer the system to a flock with the same relative positions and a different velocity, without necessarily starting the whole procedure from scratch (i.e., achieve Steps 1, 2, 3.1 again).

This can be done by quasi-static deformation (see [30] and see Section 4.3 for details) as follows. Around a flock, we have $(\alpha - \beta|v_i|^2)v_i \simeq 0$ and $F_i(x) \simeq 0$, and hence we can apply the control (7) with w as a new control, satisfying $\|w\| \leqslant M/2$, and thus focus on the simplified control system (8), as in Step 2. Take a continuous path $\tau \in [0, 1] \mapsto \bar{v}(\tau)$ satisfying $|\bar{v}(\tau)| = \sqrt{\frac{\alpha}{\beta}}$ for every $\tau \in [0, 1]$ and such that $\bar{v}(0) = \bar{v}_0$, the initial velocity of the flock, and $\bar{v}(1) = \bar{v}_1$, the velocity of the target flock. Follow the path slowly-in-time, by taking $\tau = \varepsilon t$ with $\varepsilon > 0$ small enough. Now, along this path, the simplified control system is not autonomous linear but is anyway a *slowly-varying* linear control system, obviously satisfying the Kalman condition. Then, by pole-shifting, it is possible to

design feedback controls, tracking this path and thus steering the control system, in time $1/\varepsilon$, to any point of a neighborhood of $\bar{v}_1$.

To summarize, by quasi-static deformation, we can bend the motion of the flock by moving slowly the value of $\bar{v}$ and thus steer the system to another flock. See a numerical example in Figure 2 below.

Step 3.3: Reaching mills. We now make the additional assumption that $M > M_F$. At the end of Step 1, the system is in Ω_ε. Since $v = 0$ there, we can again take the control (7) and consider w as a new control, but now, in contrast to the previous steps, since $F(x)$ will not remain small, w is subject to the constraint $\|w\| \leqslant \eta$ for some $\eta > 0$ small. We can however still focus on the simplified control system (8) near $v = 0$. It is obvious to generate feedback controls w, satisfying $\|w\| \leqslant \eta$, steering this simplified control system from any point with $v \simeq 0$ to a "mill-ready" configuration, with agents that can be equidistributed to promote a mill ring. This means that all x_i are placed along a circle of radius $R_{\rm mill}$ (where $R_{\rm mill}$ is a value of a possible mill) and where all speeds are given by $v_i = \varepsilon x_i^\perp$ for some $\varepsilon > 0$ small. This can be done either by quasi-static deformation as before, or by optimal control. Afterwards, we choose the control

$$u_i = F_i - \frac{|v_i|^2}{R_{\rm mill}} \frac{x_i}{|x_i|}$$

to ensure that each agent undergoes the correct centripetal force and moves along the circle of radius $R_{\rm mill}$. We let the system evolve and observe that $|x_i(t) - x_j(t)|$ remains constant for each pair i, j, as in Step 3.1. Moreover, v_i evolves according to

$$\dot{v}_i = (\alpha - \beta |v_i|^2) v_i - \frac{|v_i|^2}{R_{\rm mill}} \frac{x_i}{|x_i|}$$

along an heteroclinic orbit, and $v_i(t) - \sqrt{\frac{\alpha}{\beta}}\, x_i(t)^\perp \to 0$ as $t \to +\infty$, i.e., we have convergence to a mill. Such statements can be easily checked in polar coordinates.

Note that we have steered the system to a mill of which we can choose the center. Moreover, we can even steer the system to some arbitrary mill clusters: to do that, it suffices to choose appropriate "mill-ready" configurations, e.g., mill clusters that are sufficiently far one from each other.

Step 3.4: Reaching flock rings. To reach a flock ring, that is, a flock where all agents are equidistributed along a circle of radius $R_{\rm mill}$, we first proceed as in Step 3.3, except that the target velocity $v_i = \varepsilon x_i^\perp$ is replaced by $v_i = \varepsilon \bar{v}$ for some $\bar{v}$ such that $|\bar{v}| = 1$ (the desired direction of the flock). We then follow Step 3.1.

Step 3.5: Passing from any flock or mill to any other. By the same procedure as in Step 3.2, it is now clear that we can pass from any flock (or flock ring) or mill to any other, without having to restart the whole procedure at Step 1.

Step 4: Sparsification. The feedback controls defined above are not componentwise sparse, in the sense that, at any instant of time, several (usually all) components of the control are active. In order to keep a minimal amount of intervention at any instant of time, the notion of componentwise sparse control has been introduced in [17, 18] (see also [53] for the corresponding notion in infinite dimension), meaning that, at any fixed time, at most one component of the control can be active.

This notion models the action of one leader on a group of agents, like a single dog acting on a flock of sheep. It has been shown in [20] how to design, for dissipative control systems, a componentwise sparse feedbck control out of any feedback control. This can be done, for instance, by applying an averaging procedure. This is however at the unavoidable price of requiring that $M > NM_{\alpha,\beta}$. Anyway, this "sparsification" procedure is general enough to produce sparse feedback controls, steering the control system (1) from any initial condition to any flock or mill, in sufficiently large time.

We conclude with several remarks on extensions of these results.

Remark 3 (On exact controllability)**.** In Theorem 1, we have established asymptotic feedback controllability to flocks or mills. Since the linearized system around any flock or mill satisfies the Kalman condition (we are here in finite dimension), it follows that the system (1) is locally controllable around flocks and mills. Therefore, as soon as the agents are close enough to a flock (or a mill), one can always design an open-loop control steering the system in finite time exactly to the flock (or to the mill). In other words, in the framework of Theorem 1:

- Under (5), the system (1) can be steered in large time to any flock.
- Under (6), the system (1) can be steered in large time to flocks or mills.

This is a global controllability result to flocks and mills.

Remark 4 (On sharpness of the assumptions and black hole phenomenon)**.** In Theorem 1, we have assumed that the value of M is large enough. If M is too small, then it may happen that we do not have a sufficiently strong control to achieve our objectives. Given that, for certain potentials, some of the flocks or mills seem to be strongly attractive, when M is too small we may even fall in the "black hole phenomenon" (see [51]). This simply means that the attraction power of a given mill would be too strong to be countered by the control: one then cannot escape from such a basin of attraction. This consideration shows that our assumption on M is, in some sense, unavoidable. However, it is likely that, for some specific classes of potentials, the assumption can be weakened.

Remark 5 (Mean-field limit)**.** All the results in Theorem 1 related to feeback controls are still valid for smooth solutions of the mean-field PDE of Vlasov-type obtained as the formal limit $N \to +\infty$ of (1) (see [19, 53]). This is due to the fact that feedback controls are Lipschitz functions of the state (see [52]). The singular character of the flock and mill solutions as solutions of the PDE is not a difficulty since smooth solutions exist globally and only concentrate in velocity space as $t \to +\infty$. We do not provide any details.

2.2 Second main result: unbounded interactions

In Theorem 1, we have assumed that $|U'|$ is bounded. However, such an assumption does not involve the case of a potential that explodes near $r = 0$, i.e., satisfying $U(0) = -\infty$. Such potentials are often considered in collective behavior models, since they reflect the fact that two agents cannot meet: such an assumption rules out shocks. In this case, we can refine Theorem 1 as follows.

Theorem 2. *Let $U : (0, +\infty) \to \mathbb{R}$ generating a radial potential $W(x) = U(|x|)$ of class C^2 except at the origin, $\lim_{r\to+\infty} U'(r) = 0$ satisfying:*

($\mathbf{U_2}$) *Repulsiveness at 0: $\lim_{r\to 0} U'(r) = -\infty$ and for every $R > 0$ there exist a positive constant $C(R)$ such that $|U(r)| + |U'(r)| + |U''(r)| < C(R)$ for every $r \in [R, +\infty)$.*

1. *If $M > M_{\alpha,\beta}$, then the control system (1) can be steered, in sufficiently large time and with a feedback control, to any neighborhood of any flock.*

2. *Set* $\tilde{M}_F = \sup_{r>0} U'(r)$ *and* $\tilde{M}_N = \sup\{|U'(r)| : r > 2\sin(\frac{\pi}{N})\bar{R}\}$. *Under the stronger assumption* $M > \max\left(M_{\alpha,\beta} + \tilde{M}_F, \tilde{M}_N\right)$ *for some* $\bar{R} > 0$, *the control system* (1) *can be steered, in sufficiently large time and with a feedback control, from any initial condition to any neighborhood of any flock ring with radius larger than* $\bar{R}$.

3. *Under the stronger assumption* $M > \max\left(M_{\alpha,\beta} + \tilde{M}_F, \tilde{M}_N + \frac{\alpha}{\beta\bar{R}}\right)$, *for some* $\bar{R} > 0$, *the control system* (1) *can be steered to any neighborhood of any mill ring with radius larger than* $\bar{R}$.

The proof of the first statement is nearly identical to Steps 1, 2 and 3.1 of the proof of Theorem 1. Few more estimates are needed to ensure convergence of velocities and forces to 0 (see details in Section 5.1).

To prove the two last statements, the differences are more significant. Hereafter, we give a brief sketch of the strategy. Full details are given in Section 5.2. In contrast to Theorem 1, and since the potential is now infinite at 0, to prove Theorem 2 the main idea is now to a priori blow-up the group of agents, i.e. by steering them far from each other. Afterwards, we place all of them along an adequate configuration to let them converge to a flock or a mill. The first step is done by creating a fictitious potential, killing the attractive part of the initial potential U and adding a small repulsive part.

Step 1: Blow-up. In contrast to Theorem 1, the set Ω_0 may now be empty (for instance, take the potential $U(r) = 1/r$), but in the strategy that we develop below, this is actually an advantage, because in this case the Jurdjevic-Quinn strategy steers at least one of the N particles sufficiently far from all others.

Step 1.1: Fictitious purely radial potential. We apply the control

$$u_i = \frac{1}{N}\sum_{\substack{j=1\\ j\neq i}}^{N}\left(\nabla W(x_i - x_j) - \nabla\tilde{W}(x_i - x_j)\right) + w_i = F_i(x) - \tilde{F}_i(x) + w_i \tag{9}$$

which amounts to replacing in (1) the radial potential U with a new potential $\tilde{U}$, that we choose purely repulsive, satisfying (roughly speaking) $\tilde{U}' = \min(U', 0) - \eta\frac{1}{1+x^2}$. This means that we replace the potential $W(x) = U(|x|)$ with $\tilde{W}(x) = \tilde{U}(|x|)$. Hence, by choosing this control, we cancel the attractive part of the potential U and we add a small repulsive part. The constraint $\|u\| \leqslant M$ is satisfied if $\|w\| \leqslant \tilde{M}$ with

$$\tilde{M} = M - \sup_{r>0} U'(r) - 2\eta > M_{\alpha,\beta}. \tag{10}$$

In such a way, the control system (1) becomes

$$\begin{aligned} \dot{x}_i(t) &= v_i(t) \\ \dot{v}_i(t) &= (\alpha - \beta|v_i(t)|^2)v_i(t) - \tilde{F}_i(x(t)) + w_i(t) \end{aligned} \tag{11}$$

where w is the new control, subject to the constraint $\|w(t)\| \leqslant \tilde{M}$ for almost every t.

Step 1.2: Blowing-up all agents. We apply Step 1 of Theorem 1 (Jurdjevic-Quinn stabilization procedure) to the modified control system (11), in order to steer it to the set

$$\tilde{\Omega}_\varepsilon = \{(x,v) \in \mathbb{R}^{4N} \ \mid \ v = 0, \ \|\tilde{F}(x)\| < \varepsilon\}.$$

By choosing $\varepsilon > 0$ sufficiently small, we thus obtain that one of the agents is moved arbitrarily far from all others, since all forces are repulsive. Moreover, by a simple geometric observation, one can prove that this agent is also far from the convex hull of all other agents, i.e., it can be genuinely moved away from all other $N-1$ agents.

Repeating then the same strategy to all agents, one by one, we ultimately obtain that all particles can be moved far away one from each other.

Step 2: Circular equidistributed configuration. Since all agents are arbitrarily far, we have $F(x) \simeq 0$ by the assumption $\lim_{r\to+\infty} U'(r) = 0$. We can then steer all agents to a circular equidistributed configuration of large radius. The only technical detail is that we need to ensure that all particles keep being sufficiently far one from each other, so that $F(x) \simeq 0$. Details are given in Section 5.2.

Step 3: Converging to the desired target. We finally steer the configuration to the desired one as follows: we first give the desired initial impulse to the velocity variable to have either a flock ring or a mill ring with a large radius (as in the proof of Theorem 1, Step 3.1 for flock rings and Step 3.3 for mill rings). We then reduce the radius to the desired $r \geqslant \bar{R}$ by applying a suitable central force. If the target is a flock ring, we can counteract the interaction forces thanks to the assumption $M > \sup\{|U'(r)| \ \mid \ r > 2\sin(\frac{\pi}{N})\bar{R}\}$. If the target is a mill ring, we also need to counteract the centripetal force, which is possible thanks to the assumption $M > \sup\{|U'(r)| + \frac{\alpha}{\beta\bar{R}} \ \mid \ r > 2\sin(\frac{\pi}{N})\bar{R}\}$.

3 Local stability and feedback control design

In this section, we recall some known stability properties of flocks and mills established in [1, 12, 26]. These properties are useful for control design since under conditions of local stability of the corresponding flock or mill solutions, our controls can be be switched off once in a neighborhood of the profiles and the free dynamics of the system will self-regulate towards the desired limiting state. We show how to use the strategies depicted in the previous section to build feedback controls that stabilize to the flock or mill solutions.

3.1 Local stability of flock manifolds

Let us remark that the system (1) is obviously invariant under translations and rotations in space, and thus, if we find a flock solution, this particular solution gives rise to infinitely many flock solutions via these invariances. Moreover, once we have a flock solution the direction of the translational velocity of the flock can be freely chosen. It is then natural to deal with flock solutions seen as a manifold of configurations, that we describe in the following

Definition 1. Let (x^*, v^*) be an initial configuration such that the corresponding solution of (1) is a flock. The *flock manifold* associated to x^* is

$$\mathcal{F}(x^*) = \left\{ \begin{pmatrix} x \\ v \end{pmatrix} \in \mathbb{R}^{4N} \ \mid \ x \in RT(x^*), \, v = \mathbf{1}_N \otimes \bar{v}, \, \bar{v} \in \mathbb{R}^2, \, |\bar{v}| = \sqrt{\frac{\alpha}{\beta}} \right\}$$

where $RT(x^*) = \left\{ \mathbf{1}_N \otimes b + (\mathrm{Id}_N \otimes \mathcal{R}_\theta)\, x^* \;\middle|\; \theta \in [0, 2\pi),\ b \in \mathbb{R}^2 \right\}$ is the family of states obtained by rotations and translations from x^*.

The invariance of trajectories plays a crucial role in the study of solutions of (1). In particular, the concept of stability needs to be adapted to the fact that solutions do not converge to a precise point: instead, they converge to the manifold in the sense of the distance, while they go to infinity in the x-variable. For this reason, we adapt the classical definition of asymptotic convergence to this setting, by considering neighborhoods invariantly defined based on the metric. We denote by $d((x,v), A) = \inf_{a \in A} \|(x,v) - a\|$ the distance to the set $A \subset \mathbb{R}^{4N}$.

Definition 2. A manifold A is locally asymptotically stable if there exists a ε_0-neighborhood V_0 of A such that for each ε-neighborhood $V \subset V_0$ of A, there exists a δ-neighborhood U of A such that $(x(0), v(0)) \in U$ implies both $(x(t), v(t)) = (x_1(t), \dots, x_N(t), v_1(t), \dots, v_N(t)) \in V$ and $\lim_{t \to \infty} d((x(t), v(t)), A) = 0$.

The asymptotic stability of the flock manifold was analysed in [26]. There, it was shown that it is intimately related to the stability of the linearized system of the associated first-order system (3): $\dot{x}_i = F_i(x)$ with F_i given by (2), around a stationary configuration $\hat{x}$ given by $\dot{h} = G(\hat{x})h$ with

$$G_{ij}(\hat{x}) = \begin{cases} -\sum_{k \neq i} \mathrm{Hess}\, W(\hat{x}_i - \hat{x}_k) & \text{for } \ i = j, \\ \mathrm{Hess}\, W(\hat{x}_i - \hat{x}_j) & \text{for } \ i \neq j. \end{cases}$$

Under certain assumptions on the eigenvalues and eigenspaces of $G(\hat{x})$, we have a linear system $\dot{h} = G(\hat{x})h$ with a zero eigenvalue of multiplicity 4, and all other eigenvalues have a negative real part. We refer to [26, Theorem 1] for the exact assumptions needed for local asymptotically stability around the flocking manifold.

Proposition 1. *Let $\hat{x}$ be a stationary state for (3). Then, the manifold $\mathcal{F}(\hat{x})$ is locally asymptotically stable for all configurations x^* under certain assumptions on the the eigenvalues and eigenspaces of $G(\hat{x})$, in the following sense: any small enough perturbation in the variables (x, v) of the flock solution $z^* \in \mathcal{F}(\hat{x})$ associated to x^* under the dynamics (1) exponentially converges to $\mathcal{F}(\hat{x})$.*

This attractivity property of $\mathcal{F}(\hat{x})$ is natural, in view of the fact that local perturbations in (x, v) might introduce rotations and translations, that is the flock solutions are stable under small perturbations leading to another flock with a small deviation in their direction. In the following, we illustrate the use of these stability properties in conjunction with Theorem 1 to provide an effective feedback design for stabilization towards flock solutions.

3.2 Flock control with a quasi-Morse potential

Given the potential

$$W(x) = U(|x|) = V(|x|) - CV(|x|/l)\,, \qquad V(r) = -e^{-r^p/p}\,, \tag{12}$$

it is known from [25] that repulsive-attractive forces lead to a locally stable flock manifold with a particular spatial configuration. Figure 1 provides an illustration of free and controlled dynamics for this system. Given a random configuration of particles at rest (top left), the free dynamics evolve towards a ring formation which grows in time, weakening the influence of the potential (middle row). By implementing the Jurdjevic-Quinn feedback control from Theorem 1, Step 1.1, the evolution is controlled towards a bounded configuration at rest (bottom left): it corresponds

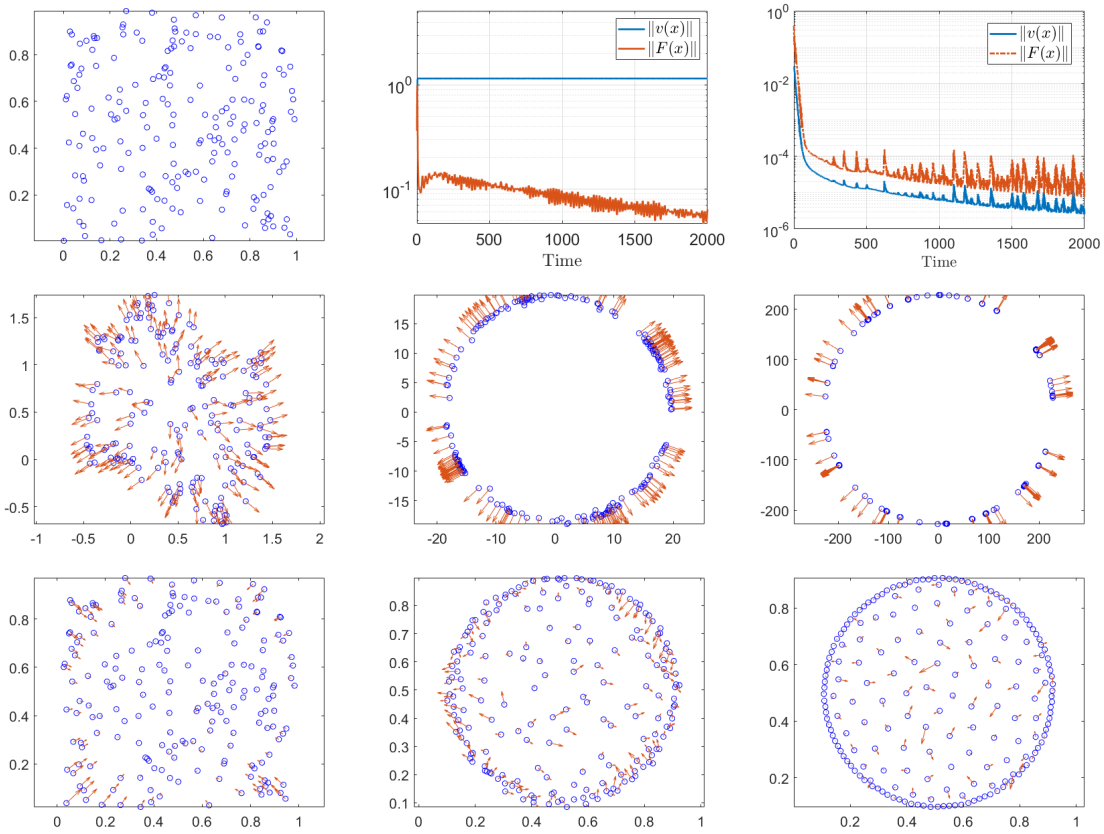

Figure 1: Jurdjevic-Quinn stabilization for the quasi-Morse potential (12) with $C = 0.6, p = 1.5$, $l = 0.5, \alpha = 2, \beta = 1.5, N = 200$. From left to right. Top: initial state, uncontrolled and controlled energy evolution. Middle: uncontrolled evolution at $t = 4, 20, 200$. Bottom: controlled evolution at $t = 4, 20, 200$. The Jurdjevic-Quinn feedback law stabilizes towards a neighborhood of Ω_ϵ.

to the locally stable uncontrolled profile found in [25]. The uncontrolled dynamics then converge towards a state where $\|F(x)\| = 0$ due to expansion, while $\|v(x)\|$ remains constant because of self-propulsion (top, middle). Instead, the Jurdjevic-Quinn stabilization ensures decay on both quantities (top, right), generating a configuration that can be subsequently stabilized towards different flocks (bottom middle, right).

In Figure 2, we illustrate the quasi-static deformation between different flocks pointing towards different directions using the strategy of Step 3.2 of the previous section. Given a time horizon T, initial and terminal velocities v_0 and v_T, characterized by angles θ_0 and θ_T respectively, and magnitude $\sqrt{\frac{\alpha}{\beta}}$, we transition from v_0 to v_T through the action of the linear, time-dependent, feedback control

$$u_i(v_i, t) = -M(v_i - \mathcal{R}_{\theta(t)} v_0)\,, \quad \theta(t) = \theta_0 + \frac{t}{T}(\theta_T - \theta_0)\,, \tag{13}$$

where $\mathcal{R}_\theta$ is the rotation matrix.

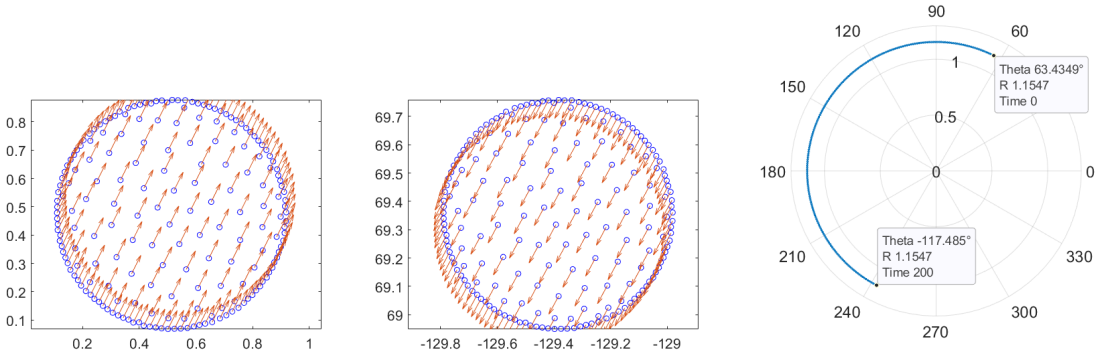

Figure 2: Quasi-static deformation for flock transition with a quasi-Morse potential (12) with $C = 0.6$, $p = 1.5, l = 0.5, \alpha = 2, \beta = 1.5, N = 200$. Left: initial flock. Middle: terminal flock. Right: average angle evolution. The use of the quasi-static feedback law (13) connects different flocks.

3.3 Local stability of mill rings

We now turn our attention to the study of the local behavior of mill rings. We introduce adapted coordinates, and study the asymptotic stability for solutions exhibiting rotational symmetries only. It is then useful to introduce the time-varying orthonormal frame in $\mathbb{R}^{2N}$

$$e_i^r = \left(\cos\left(\frac{2\pi i}{N} + \omega t\right), \sin\left(\frac{2\pi i}{N} + \omega t\right)\right), \qquad e_i^\perp = (e_i^r)^\perp,$$

with $e^\perp$ denoting the rotated vector by $\pi/2$ of $e \in \mathbb{R}^2$, and ω the angular velocity of the mill. Without loss of generality, we consider a mill ring of N agents rotating around the point $(0, 0)$. By rearranging indices, we assume that positions and velocities satisfy

$$x_i(t) = Re_i^r, \qquad v_i(t) = \sqrt{\frac{\alpha}{\beta}} e_i^\perp.$$

for $i = 1, \dots, N$. It is clear that $\dot{e}_i^r = \omega e_i^\perp$ and $\dot{e}_i^\perp = -\omega e_i^r$. The mill radius R is given by the solution of (4). We now consider a perturbation around such a mill solution, that we write as

$$x_i(t) = (R + r_i(t))\mathcal{R}_{\theta_i(t)} e_i^r, \qquad v_i(t) = \left(\sqrt{\frac{\alpha}{\beta}} + w_i(t)\right) \mathcal{R}_{\tau_i(t)} e_i^\perp.$$

A straightforward computation shows that the system (1) can be written in term of the polar variable $r_i, \theta_i, w_i, \tau_i$. A general result of stability around such solutions seems out of reach (see some results for a first-order system with a similar structure in [12]). We instead briefly investigate the local stability of solutions with rotational symmetries, i.e., solutions that satisfy $r_i = r_j, \theta_i = \theta_j, w_i = w_j, \tau_i = \tau_j$ with $i, j = 1, \dots, N$. Notice that due to the rotational symmetry, the last equation becomes $\dot{\tau}_i = -\omega$. By dropping the index for variables r_i, w_i and introducing the variable $\gamma = \theta_i - \tau_i$, the system is reduced to

$$\begin{aligned} \dot{r} &= \left(\sqrt{\frac{\alpha}{\beta}} + w\right) \sin(\gamma), \qquad \dot{\gamma} = \left(\frac{\sqrt{\frac{\alpha}{\beta}} + w}{R + r} - \frac{\phi(r)}{\sqrt{\frac{\alpha}{\beta}} + w}\right) \cos(\gamma), \\ \dot{w} &= -\left(2\sqrt{\alpha\beta} w + \beta w^2\right)\left(\sqrt{\frac{\alpha}{\beta}} + w\right) - \phi(r)\sin(\gamma), \end{aligned} \tag{14}$$

where

$$\begin{aligned}\phi(r) &= (1,0)\cdot\frac{1}{N}\sum_{j=1}^{N-1}\nabla W\left((R+r)((1,0)-\left(\cos\left(\frac{2\pi j}{N}\right),\sin\left(\frac{2\pi j}{N}\right)\right)\right)\\ &= \frac{1}{N}\sum_{j=1}^{N-1}\sin\left(\frac{\pi j}{N}\right)U'\left((R+r)\sin\left(\frac{\pi j}{N}\right)\right).\end{aligned}$$

Note that, since (4) is satisfied, we have $\frac{\sqrt{\frac{\alpha}{\beta}}}{R}=\frac{\phi(0)}{\sqrt{\frac{\alpha}{\beta}}}=\omega$. In particular, the trajectory $(r(t),\gamma(t),w(t))=(0,0,0)$ is a solution of (14). This shows invariance of the mill solution under a same translation in all variables α_i,β_i. One can easily study linear stability properties for (14): the linearized system is given by

$$\begin{pmatrix}\dot r\\ \dot\gamma\\ \dot w\end{pmatrix}=\begin{pmatrix}0 & \sqrt{\frac{\alpha}{\beta}} & 0\\ -\frac{\omega}{R}-\frac{\phi'(0)}{\sqrt{\frac{\beta}{\alpha}}} & 0 & \frac{2}{R}\\ 0 & -\phi(0) & -2\alpha\end{pmatrix}\begin{pmatrix}r\\ \gamma\\ w\end{pmatrix}.$$

Recalling that $\alpha,\beta,\phi(0)>0$, linear stability is ensured by the condition $\frac{\omega}{R}+\frac{\phi'(0)}{\sqrt{\frac{\beta}{\alpha}}}>0$. This condition is always satisfied for power-law potentials of the form

$$U(s)=\frac{|s|^a}{a}-\frac{|s|^b}{b},\qquad a>b>0,\tag{15}$$

since we have in this case

$$\phi'(0)=\sqrt{\frac{\alpha}{\beta}}\omega(a-b)R^b\sum_{j=1}^{N-1}\sin\left(\frac{\pi j}{N}\right).$$

This linear stability analysis shows that the equilibrium solution $(r(t),\gamma(t),w(t))=(0,0,0)$, i.e., the mill ring solution is a locally asymptotically stable equilibrium point to (14). As a consequence, the mill ring solution is locally asymptotically stable for perturbations keeping the rotational symmetry of (1). In the following, we explore the interplay between stability of mill rings and control design for power law potentials.

3.4 Controlling mills for a power-law potential

Although the local stability analysis is enough for our purposes of controlling the system (1) towards mill ring solutions, we observe that for power-law potentials (15), the mill ring is globally asymptotically stable for solutions with rotational symmetry. Figure 3 (top row) shows the evolution of a particular solution, not a small perturbation, with rotational symmetry, converging towards a stable mill with radius given by (4), similar to a nonlinear damped oscillator. The second row further illustrates the stability of the mill ring by considering the evolution of two types of perturbations. On the left, the initial configuration is a mill ring with radius different from the stable solution. On the right, the initial configuration is a ring of stable radius, however the tangential velocities are shifted by an angle γ_0. In both plots, the vertical axis represents the distance with respect to the stable radius, and we can observe that for both types of perturbations the uncontrolled dynamics stabilize towards the mill.

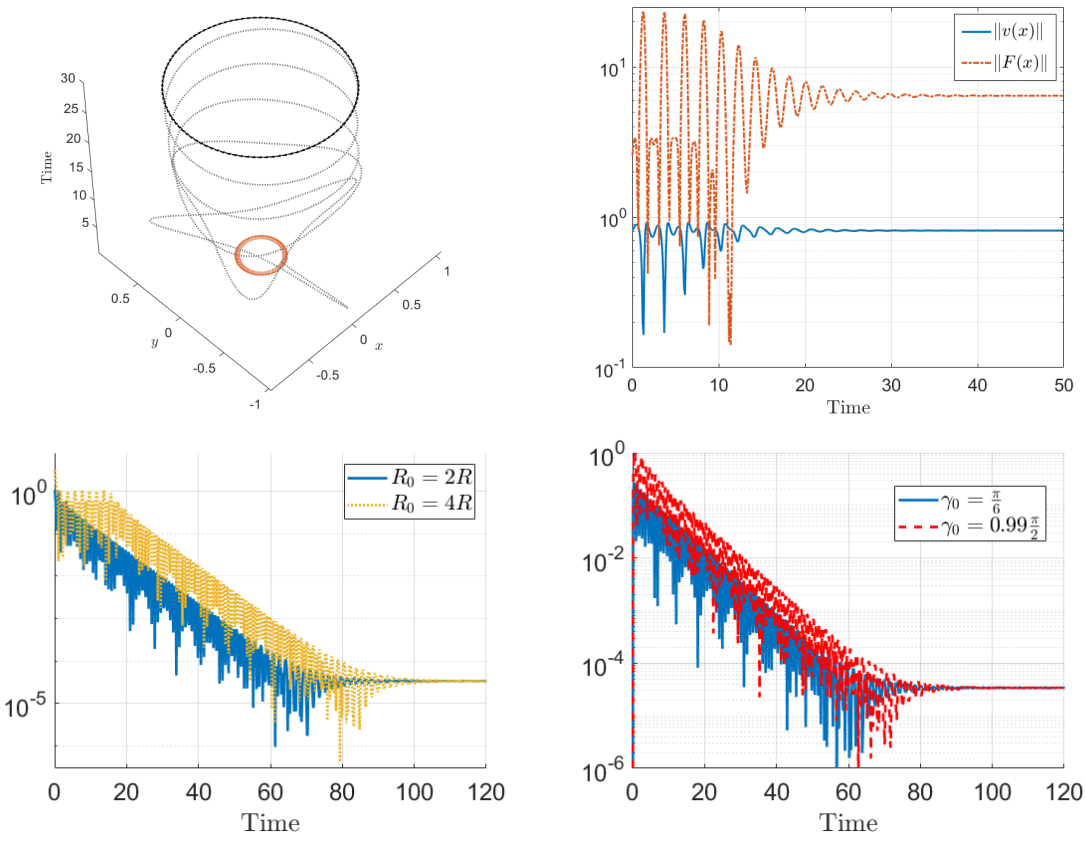

Figure 3: Mill ring stability in the power-law potential (15) with $a = 4, b = 1, \alpha = 10, \beta = 3$, $N = 200$. Top left: an initial ring configuration converges to mill ring solution (sample agent trajectory in grey). Top right: energy evolution of the swarm towards the mill. Bottom left: evolution of the distance to the stable mill radius R for mill configurations departing from an initial radius R_0. Bottom right: evolution of the distance to stable mill radius for rings of radius R, initial velocity rotated from the tangential velocity by γ_0. The evolution to the stable mill configuration is robust to perturbations.

Feedback controls can be used to induce or accelerate convergence to mill ring solutions. For example, given a stable flock ring configuration, the system can be stabilized towards a mill through the action of the feedback law

$$u_i(v_i(t)) = -M\left(x_i, v_i - \sqrt{\frac{\alpha}{\beta}}\frac{x_i^\perp}{|x_i^\perp|}\right).$$

A design alternative is to resort to instantaneous controls [6], which can be interpreted as feedback laws in the same spirit of model predictive control strategies. We synthesize a feedback control by solving

$$\min_{u\in[-1,1]^2} \sum_{i=1}^{N} \left| v_i - \sqrt{\frac{\alpha}{\beta}}\frac{x_i^\perp}{|x_i^\perp|^2}\right| + (|x_i - x_m|^2 - R_m^2)^2 + \lambda_1|u| + \lambda_2|u|^2\,, \quad \lambda_1, \lambda_2 > 0\,, \tag{16}$$

where x_m corresponds to the center of mass of the swarm, R_m is the desired mill radius, and (x_i, v_i) is the future state of the system after a small control horizon Δt. We consider ℓ_1 and ℓ_2-norm control penalties to induce sparsification in time. For the sake of real-time computability, this optimization is reduced to a single control signal $u \in \mathbb{R}^2$, which enters the dynamics through an incremental rotation of $\frac{2\pi}{N}$. This control differs from the signal that would be obtained optimizing each u_i separately, however it still succeeds in stabilizing around the mill ring solution, as shown in Figure 4, presumably due to the large basin of attraction surrounding the mill ring solution.

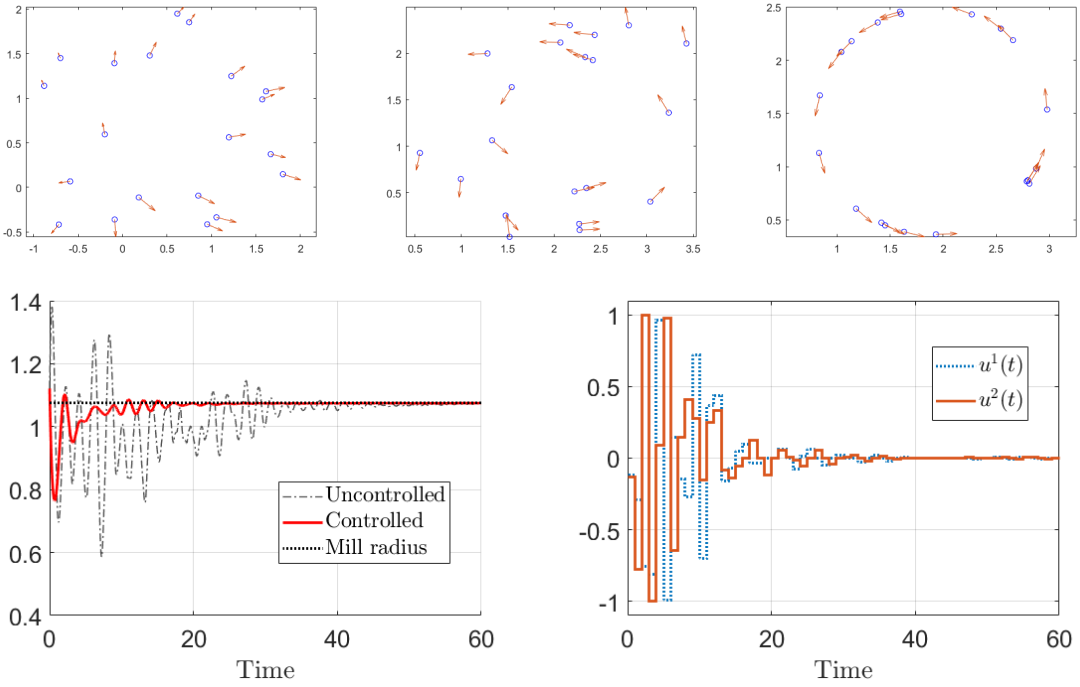

Figure 4: Stabilization towards a mill ring for the power-law potential (15) with $a = 4, b = 1$, $\alpha = 10, \beta = 3$, $N = 20$, using the feedback (16). Top (left to right): swarm at $t = 0, 10, 40$. Bottom left: evolution of the configuration radius towards the stable mill. Bottom right: control signal.

We apply a similar idea to control a stable mill towards a flocking configuration of different radius. In this case we compute one control variable per agent by solving

$$\min_{u\in[-1,1]^{2N}} \sum_{i=1}^{N} |v_i - \bar{v}|^2 + (|x_i - x_m|^2 - R_f^2)^2 + \lambda |u_i|^2 \,, \quad \lambda > 0 \,, \tag{17}$$

where $\bar{v}, R_f$ are the desired flocking velocity and radius, respectively. Figure 5 illustrates the transition from the milling to the flocking regime.

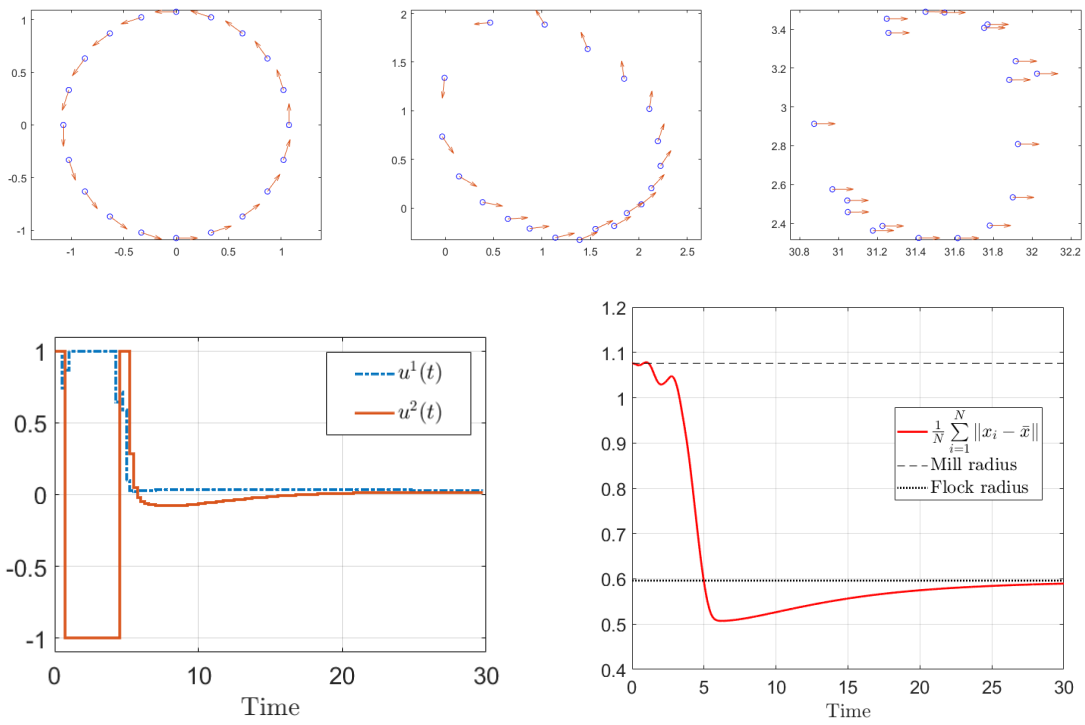

Figure 5: Controlled transition from mill to flock for the power-law potential ($a = 4, b = 1, \alpha = 10, \beta = 3, N = 20$), using the feedback (17). Top: swarm at $t = 0, 4, 40$. Bottom left: a sample control signal. Bottom right: evolution of the swarm radius, from a stable mill to a stable flock.

4 Proof of Theorem 1

This section is devoted to provide the full detail of the proof of Theorem 1, sketched in Section 2.1.

4.1 Proof of Step 1

In this first step, the goal is to steer the control system from any initial point to a point in Ω_ε.

Step 1.1. Jurdjevic-Quinn stabilization

Let $\gamma > \max\left(1, \frac{1}{M}\sqrt{\frac{\alpha^3}{\beta}}\right)$ be fixed. We apply the feedback control

$$u_i(v_i) = \begin{cases} 0 & \text{if } |v_i| \geqslant 2\gamma\sqrt{\frac{\alpha}{\beta}}, \\ -M\frac{v_i}{|v_i|}\left(2 - \frac{|v_i|}{\gamma\sqrt{\frac{\alpha}{\beta}}}\right) & \text{if } |v_i| \in \left(\gamma\sqrt{\frac{\alpha}{\beta}}, 2\gamma\sqrt{\frac{\alpha}{\beta}}\right), \\ -M\frac{v_i}{|v_i|} & \text{if } |v_i| \in \left[\frac{\sqrt{\frac{\alpha}{\beta}}}{\gamma}, \gamma\sqrt{\frac{\alpha}{\beta}}\right], \\ -M\frac{\gamma}{\sqrt{\frac{\alpha}{\beta}}}v_i & \text{if } |v_i| < \frac{\sqrt{\frac{\alpha}{\beta}}}{\gamma}. \end{cases} \tag{18}$$

Since the control is Lipschitz with respect to the (x, v) variables, we have existence and uniqueness of solutions of (1) for a fixed initial condition. Note that the control law satisfies the constraint $|u_i| \leqslant M$ by construction. Setting the total energy of the system as

$$V(t) = \frac{1}{2}\sum_{i=1}^{N} |v_i(t)|^2 + \frac{1}{2}\sum_{\substack{i,j=1 \\ i\neq j}}^{N} W(x_i(t) - x_j(t)),$$

using (1), we have

$$\dot{V} = \sum_{i=1}^{N} v_i \cdot \dot{v}_i + \frac{1}{2}\sum_{\substack{i,j=1 \\ i\neq j}}^{N} \nabla W(x_i - x_j)(\dot{x}_i - \dot{x}_j) = \sum_{i=1}^{N} \left((\alpha - \beta|v_i|^2)|v_i|^2 + v_i \cdot u_i\right).$$

Notice that by skew-symmetry of $\nabla W(x_i - x_j)$, we have

$$\sum_{\substack{i,j=1 \\ i\neq j}}^{N} \nabla W(x_i - x_j) \cdot v_j = -\sum_{\substack{i,j=1 \\ i\neq j}}^{N} \nabla W(x_i - x_j) \cdot v_i \,.$$

Given $a_1 = \frac{1}{\gamma}\sqrt{\frac{\alpha}{\beta}}$ and $a_2 = \gamma\sqrt{\frac{\alpha}{\beta}}$, we split the indices $i = 1, \dots, N$ in the sets

$$I_\infty(t) = \{i : |v_i(t)| > a_2\}\,,\ I_1(t) = \{i : |v_i(t)| \in [a_1, a_2]\} \text{ and } I_0(t) = \{i : |v_i(t)| < a_1\}\,.$$

Apply the control law (18) and notice that for every $i \in I_\infty(t)$ we obtain

$$\left\{ v_i \cdot u_i = 0 \quad \text{or} \quad v_i \cdot u_i = -M|v_i|\left(2 - \frac{|v_i|}{\gamma\sqrt{\frac{\alpha}{\beta}}}\right) < 0 \right\} \quad \text{and} \quad (\alpha - \beta|v_i|^2)|v_i|^2 < 0.$$

We deduce

$$\dot{V} \leqslant \sum_{i\in I_\infty(t)} (\alpha - \beta|v_i|^2)|v_i|^2 + \sum_{i\in I_1(t)} |v_i|(\alpha|v_i| - \beta|v_i|^3 - M) + \sum_{i\in I_0(t)} \left(\alpha - \beta|v_i|^2 - M\frac{\gamma}{\sqrt{\frac{\alpha}{\beta}}}\right)|v_i|^2.$$

The maximum of the function $v \to \alpha v - \beta v^3$ over $v \geqslant 0$ is $\sqrt{\frac{4\alpha^3}{27\beta}} < M$. We have $\alpha|v_i| - \beta|v_i|^3 - M < 0$ and $\alpha - M\frac{\gamma}{\sqrt{\frac{\alpha}{\beta}}} < 0$ by the choice of γ. This implies that

$$\dot{V} \leqslant \sum_{i\in I_\infty(t)} (\alpha - \beta|v_i|^2)|v_i|^2 - \sum_{i\in I_1(t)\cup I_0(t)} \beta|v_i|^4. \tag{19}$$

The right-hand side is then nonpositive being the sum of two nonpositive terms, hence $\dot{V} \leqslant 0$. Note that we cannot directly apply the LaSalle invariance principle to the system, because we cannot ensure boundedness of the trajectories and the functional V is not proper.

Nevertheless, V is bounded below, since both $|v|$ and W are bounded below, as a consequence of the corresponding assumption on U. Since $V(t)$ is decreasing, hence bounded above, both $v_i(t)$ and $W(x_i(t) - x_j(t))$ are bounded. Thanks to the assumption ($\mathbf{U_1}$), ∇W is bounded. This implies that $\dot{v}_i(t)$ is bounded too.

Lemma 1. We have $\lim_{t\to+\infty} v_i(t) = 0$ for $i = 1, \dots, N$.

Proof. By contradiction, if this is not the case, there exists an index i and a sequence of times $t_k \to \infty$ such that $|v_i(t_k)| > C$. Since $\dot{v}_i$ is bounded, this implies that there exists a uniform τ such that $|v_i(t)| > C/2$ for all $t \in (t_k - \tau, t_k + \tau)$. By using this property in (19) discarding the first term in the right-hand side, we infer that $V(t) \to -\infty$. This raises a contradiction. □

Lemma 2. We have $\lim_{t\to+\infty} F_i(x(t)) = 0$ for $i = 1, \dots, N$.

Proof. Since the v_i are bounded, then the functions $x_i(t) - x_j(t)$ are Lipschitz. Since ($\mathbf{U_1}$) holds, then both $\nabla W(x_i(t_k) - x_j(t_k))$ and its derivative are bounded; hence functions $\nabla W(x_i(t) - x_j(t))$ are Lipschitz too, with a Lipschitz constant that we denote with L.

Assume now, by contradiction, that there exists an index i such that $F_i(x(t))$ does not converge to 0. Thus, there exists a sequence of times $t_k \to \infty$ such that

1. either $F_i(x(t)) \to \bar{F}$ for some non-zero vector $\bar{F}$;
2. or $|F_i(x(t))| \to +\infty$.

In the first case, for each $\varepsilon > 0$ there exists an index $K > 0$ such that $\|F_i(x(t)) - \bar{F}\| < \varepsilon + L(t - t_k)$ for all $k > K$ and $t > t_k$. Recalling that $\lim_{t\to+\infty} v_i(t) = 0$, take now $\eta > 0$ sufficiently small and k sufficiently large to have both $|v_i(t)| < \eta$ and $|\alpha v_i(t) - \beta v_i(t)|v_i(t)|^2| < \eta$ for all $t > t_k$. This implies $|\dot{v}_i(t_k + \tau) - \bar{F}| < 2\eta + L\tau$ for all $\tau > 0$. Since $|v_i(t_k)| < \eta$, then $|v_i(t_k + \tau) - \bar{F}\tau| < \eta + 2\eta\tau + L\frac{\tau^2}{2}$ for $\tau > 0$. Fix $\tau > 0$ sufficiently small to have $L\frac{\tau^2}{2} < |\bar{F}|\frac{\tau}{2}$ and observe that this implies $|v_i(t_k + \tau)| > |\bar{F}|\frac{\tau}{2} - \eta - 2\eta\tau$. Let $\eta \to 0$ and note that this implies $\lim_{k\to\infty} v_i(t_k + \tau) \neq 0$. This raises a contradiction.

The second case is similar: consider the unit vectors $\frac{F_i(x(t))}{|F_i(x(t))|}$, that admit a converging subsequence (that we do not relabel) to an unitary vector $\bar{F}$. Following computations of the previous case, we have $|v_i(t_k + \tau)| > |F_i(x(t_k))|\frac{\tau}{2} - \eta - 2\eta\tau$, which does not converge to 0 for $\eta \to 0$ and $k \to \infty$. This raises a contradiction. □

Finally, let us choose a time T_0 at which we stop the control strategy (18). This choice is driven by correctly initializing the next step. Let $\varepsilon' > 0$ be a constant to be chosen later. Since both $v_i(t)$ and $F_i(x(t))$ converge to 0, we choose a time T_0 at which $|v_i(T_0)| < \varepsilon'$ and $|F_i(x(T_0))| < \varepsilon'$ for $i = 1, \dots, N$.

Step 1.2. Reaching Ω_ε in finite time

We now steer each v_i exactly to zero. Choose $T_{1,i} = T_0 + \frac{1}{\varepsilon'}|v_i(T_0)|$ and define

$$v_i(t) = \begin{cases} v_i(T_0) - \varepsilon'(t - T_0)\frac{v_i(T_0)}{|v_i(T_0)|} & \text{for } t \in [T_0, T_{1,i}], \\ 0 & \text{for } t > T_{1,i}. \end{cases}$$

Then choose $T_1 = \max(T_{1,i})$ as the final time of the strategy. A direct computation shows that

$$|x_i(t) - x_i(T_0)| \leqslant \int_{T_0}^{T_{i,1}} |v_i(T_0)| - \varepsilon'(t - T_0)\, dt \leqslant \frac{|v_i(T_0)|^2}{2\varepsilon'} < \frac{\varepsilon'}{2} \tag{20}$$

for every $t \in [T_0, T_1]$. Since $\nabla W(x_i - x_j)$ is L-Lipschitz, as recalled in Lemma 2, we infer that $\|F_i(T_0 + t)\| \leqslant \|F_i(T_0)\| + L\frac{\varepsilon'}{2} < (1 + \frac{L}{2})\varepsilon'$. This implies that $(x(T_1), v(T_1)) = (\bar{x}, 0) \in \Omega_\varepsilon$ by imposing $\varepsilon' \leqslant \varepsilon/(1 + \frac{L}{2})$. The control satisfies

$$|u_i| \leqslant |\dot{v}_i| + (\alpha - \beta|v_i|^2)|v_i| + |F_i| < \varepsilon' + \alpha\varepsilon' + (1 + \tfrac{L}{2})\varepsilon' \leqslant M$$

by imposing $\varepsilon' \leqslant M/(2+\alpha+\frac{L}{2})$. Summing up, choosing $\varepsilon' = \min\left(\frac{\varepsilon}{1+\frac{L}{2}}, \frac{M}{2+\alpha+\frac{L}{2}}\right)$, all conditions are satisfied.

4.2 Proof of Step 2

Step 2 is obvious, the control system (8) being straightforward to control. We do not provide any detail.

4.3 Proof of Step 3

Step 3.1: Reaching flocks

Fix a unit vector $\bar{v}$ and note that the configuration $(\bar{x}, \frac{\delta}{2}\bar{v})$ belongs to the δ-neighborhood of $(\bar{x}, 0)$. Then, we can steer the system from $(\bar{x}, 0)$ to $(\bar{x}, \frac{\delta}{2}\bar{v})$ at a time $T_2 > T_1$ with a control $u = \bar{u} + z$ satisfying $\|u\| < 2\varepsilon < M$, again by a local controllability argument.

We then choose the controls $u_i = F_i$ on the time interval $[T_2, +\infty)$. The velocity variables are then the solutions of

$$\dot{v}_i(t) = (\alpha - \beta|v_i(t)|^2)v_i(t), \qquad v_i(T_2) = \tfrac{\delta}{2}\bar{v}. \tag{21}$$

They all coincide at each time, i.e., $v_i(t) = v_j(t)$, hence relative positions are all constant with respect to time, i.e $x_i(t) - x_j(t) = \bar{x}_i - \bar{x}_j$. This in turn implies that interaction forces keep being constant with respect to time, thus $\|u_i(t)\| = \|F_i(t)\| = \|F_i(T_2)\| < \varepsilon$, since $(x(T_2), v(T_2)) \in \Omega_\varepsilon$.

Moreover, all velocities converge to $\sqrt{\frac{\alpha}{\beta}}\bar{v}$ for $t \to +\infty$, since they solve (21). This implies that the system converges to an ε-flock, as stated.

Remark 6. The motion of the velocity variables $v_i(t)$, solutions of (21), exactly follows *heteroclinic trajectories*, in the sense that $v_i(t)$ passes from (a neighborhood of) the unstable equilibrium 0 to the asymptotically stable family of equilibria $\left\{\|v\| = \sqrt{\frac{\alpha}{\beta}}\right\}$. The existence of such heteroclinic trajectories is certainly one of the main interesting features of the dynamics of (1), promoting convergence to flocks or mills.

Step 3.2: Passing from a flock to another flock

Assume that the system is at (or near) a flock of velocity $\bar{v}_0$. We want to steer the system to another flock, of velocity $\bar{v}_1$. Along the motion, the relative positions $x_i - x_j$ will remain constant.

The strategy that we use here is by *quasi-static deformation*. Take a continuous path $\tau \in [0,1] \mapsto \bar{v}(\tau)$ such that $\bar{v}(0) = \bar{v}_0$ and $\bar{v}(1) = \bar{v}_1$, satisfying $\|v(\tau)\| = \sqrt{\frac{\alpha}{\beta}}$ for every $\tau \in [0,1]$, e.g., the shortest arc on the circle. Since relative positions do not change, forces F_i do not change and then, for each τ, we have a flock of velocity $\bar{v}(\tau)$.

Of course, the corresponding path of flocks, parametrized by $\tau \in [0,1]$ is *not* a solution of (1). It is rather to be thought of as a path of equilibrium points for the dynamics (1). Following the idea of [30, 31], we track this path, in large time, by designing appropriate feedback controls. To this aim, we set $\tau = \varepsilon t$, for some $\varepsilon > 0$ small enough, and $t \in [0, 1/\varepsilon]$. Of course, for every fixed value of τ, the control system (8) is linear autonomous, of the form $\dot{X}(t) = AX(t) + Bu(t)$ for some matrices A and B. It obviously satisfies the Kalman condition and is thus controllable and also feedback stabilizable (for instance by standard pole shifting, see e.g. [46, 55, 57]). But now, along the path of flocks, we do not have anymore a linear autonomous control system, but a linear *instationary* control system, of the form $\dot{X}(t) = A(t)X(t) + B(t)u(t)$ for some matrices $A(t)$ and $B(t)$ depending on time. For every time t, the pair $(A(t), B(t))$ still satisfies the Kalman condition. However, as

it is well known, for linear instationary control systems the Kalman condition is not sufficient to ensure controllability nor stabilizability properties (see counterexamples, e.g., in [41, 55, 57]). The idea raised in [30] is on the contrary to follow the path slowly in time: by setting $\tau = \varepsilon t$, the abovementioned control system takes the form $\dot{X}(t) = A(\varepsilon t)X(t) + B(\varepsilon t)u(t)$ and is therefore a *slowly-varying* (in time) linear control system, still satisfying the Kalman condition. As explained in detail in [30], and according to an argument of [41], if $\varepsilon > 0$ is small enough then the Kalman condition is still sufficient to ensure that this slowly-varying linear control system can be feedback stabilized by usual pole shifting, with a feedback control of the form $u(t) = K(\varepsilon t)X(t)$. Note anyway that such a feedback is also slowly varing in time, so is not a "pure" feedback. One may want to obtain a feedback, not depending on time, but defined piecewise in time. This is possible by slightly modifying the above definition of the feedback. The resulting *staircase method* has been used e.g. in [54].

Eventually, such feedback controls make it possible to track the path of flocks and thus steer the control system, in time $1/\varepsilon$, to any point of a neighborhood of $\bar{v}_1$.

If one moreover aims to choose precise x-positions (keeping anyway the same relative positions as those of the initial flock), it is sufficient to observe that all such configurations differ from a translation vector X. Therefore, it suffices to use a quasi-static deformation on the positions as well.

Proof of Steps 3.3, 3.4, 3.5: reaching mills, flock rings

The strategy, described in Section 2.1, is similar to what has been described above, and we thus do not give any detail.

5 Proof of Theorem 2

5.1 Proof of the first statement

The proof of the first statement is almost identical to the proof of Theorem 1, with the following differences:

- In Step 1.1, we follow the proof until $\dot{V} \leqslant 0$, due to (19). Since V is bounded below, both v_i and $W_i(x_i - x_j)$ are bounded below. Now, using the assumptions ($\mathbf{U_2}$), boundedness of W implies that $x_i(t) - x_j(t)$ is bounded away from 0 by a constant $2\ell > 0$, hence $\nabla W(x_i(t) - x_j(t))$ is bounded. This in turn implies that $\dot{v}_i(t)$ is bounded as well. One can then prove Lemmas 1 and 2 in this case too.
- In Step 1.2, we observe that (20) ensures that $|x_i(t) - x_j(t)| > \ell$, provided $\varepsilon' < \sqrt{2\ell}$. We then use ($\mathbf{U_2}$) to ensure that ∇W is L-Lipschitz for $|x_i(t) - x_j(t)| > \ell$. We now choose $\varepsilon' = \min(\sqrt{2\ell}, \frac{2}{L}, \frac{\varepsilon}{2})$ to ensure that $(x(T_1), v(T_1)) \in \Omega_\varepsilon$.

5.2 Proof of the second statement

We follow the sketch of the proof given in Section 2.2.

5.2.1 Proof of Step 1

Step 1.1: Fictitious purely radial potential. The proof is based on the method of "artificial potential field", which is widely used in robotics (see, e.g., [56, Chap. 7]). Replace the potential U with a purely repulsive potential $\tilde{U}$, that is defined below. Here, by replacing U' with $\min(U'(x), 0)$ we cancel the attractive part.

We define

$$\eta = \frac{1}{4}\left(M - \sqrt{\frac{4\alpha^3}{27\beta}} - \sup_{r>0} U'(r)\right) > 0$$

$$U^+(x) = \min(U'(x), 0) - \eta\frac{1}{1+x^2}, \qquad U^-(x) = \min(U'(x), 0) - 2\eta\frac{1}{1+x^2}.$$

We choose $\tilde{U}'$ as a C^∞ function satisfying $U'(x) \in (U^-(x), U^+(x))$ for all $x \in (0, +\infty)$. Such a function $\tilde{U}'$ exists, since C^∞ is dense in C^0 and $U^+, U^- \in C^0$. Hence,

$$\sup_{r>0} |\tilde{U}'(r) - U'(r)| \leqslant \sup_{r>0} U'(r) + 2\eta\,. \tag{22}$$

It is easy to prove that $\tilde{U}(x) = \int_1^x \tilde{U}'(x)$ satisfies ($\mathbf{U_2}$), by construction. Define now $\tilde{W}(x) = \tilde{U}(x)$ and choose the control $u_i = F_i(x) + \tilde{F}_i(x) + w_i$ (see (9)), so that the new control system is (11), with the new controls w_i satisfying $\|w_i\| \leqslant \tilde{M}$ with $\tilde{M}$ defined by (10). Note that (22) implies that

$$\|u_i\| \leqslant \left\|F_i(x) - \tilde{F}_i(x)\right\| + \|w_i\| \leqslant \sup_{r>0} |U'(r) - \tilde{U}'(r)| + \tilde{M} \leqslant \sup_{r>0} U'(r) + 2\eta + \tilde{M} = M,$$

i.e., the control constraint is satisfied.

Step 1.2: Blowing-up all agents. Fix $\varepsilon > 0$ to be chosen later. Applying Step 1 of Theorem 1 to the control system (11), we can steer it to $\tilde{\Omega}_\varepsilon = \{(x, v) \;|\; v = 0,\ \|\tilde{F}(x)\| < \varepsilon\}$ in finite time T_0. The crucial observation here is that $\tilde{U}'(x) < U^+(x) \leqslant -\eta\frac{1}{1+x^2}$, i.e., all forces are purely repulsive. We now study the configuration $(x(T_0), v(T_0)) = (\bar{x}, 0) \in \tilde{\Omega}_\varepsilon$. Since it is a configuration of N agents in the plane, the convex closure of positions $(x_1, \dots, x_N)$ is a polygon of $n \leqslant N$ vertices, in which at least one of the internal angles is smaller than $\frac{n-2}{n}\pi$, thus smaller than $\frac{N-2}{N}\pi$.

By relabelling indices, we assume that x_N is one of those vertices. By a simple geometrical observation, all interaction forces point outwards of the polygon (see Figure 6). More precisely,

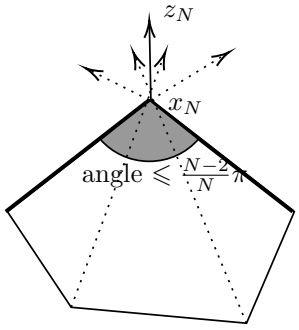

Figure 6: The outer vector z_N.

consider z_N to be the unit vector in the direction of the outer angle bisector and note that each component of the force $\tilde{F}_{Nj} = \frac{1}{N}\nabla\tilde{W}(\bar{x}_N - \bar{x}_j)$ satisfies

$$\tilde{F}_{Nj} \cdot z_N \geqslant \frac{1}{N}|\tilde{U}'(|\bar{x}_N - \bar{x}_j|)|\cos(\tfrac{N-2}{2N}\pi).$$

This in turn implies that

$$\|\tilde{F}_N\| \geqslant \tilde{F}_N \cdot z_N \geqslant \tfrac{1}{N}\sup_{j\neq N}|\tilde{U}'(|\bar{x}_N - \bar{x}_j|)|\cos(\tfrac{N-2}{2N}\pi) \geqslant \tfrac{1}{N}\eta\frac{\cos(\frac{N-2}{2N}\pi)}{1 + \inf_{j\neq N}|\bar{x}_N - \bar{x}_j|^2}.$$

Choose now an arbitrarily large distance $L > 1$ and set $\varepsilon = \frac{\eta}{N(1+L^2)} \cos(\frac{N-2}{2N}\pi)$. The condition $(\bar{x}, 0) \in \tilde{\Omega}_\varepsilon$ implies $\|F_N\| < \varepsilon$, hence $|x_N - x_j| > L$ for all $x \neq N$.

Since the distance between x_N and the other agents is arbitrarily large and $\lim_{r\to\infty} \tilde{U}'(r) = 0$, the components $\tilde{F}_{Nj}$ and $\tilde{F}_{jN}$ of the forces are arbitrarily small. Hence, all configurations $((\bar{x}_1, \dots, \bar{x}_{N-1}, \bar{x}_N + \tau_N z_N), 0)$ with $\tau_N > 0$ belong to $\tilde{\Omega}_\varepsilon$. By quasi-static deformation, we can steer $\bar{x}_N$ arbitrarily far from the other $\bar{x}_i$'s along the direction z_N, by choosing τ_N sufficiently large.

We next apply the same strategy to the remaining $N-1$ agents and we steer one of them away from all others, while keeping x_N arbitrarily far, due to the choice of τ_N. We repeat the procedure to the remaining $N-2$ agents, while keeping both x_{N-1}, x_N sufficiently far, and so forth. In finite time, we are able to steer all agents to a configuration $(\bar{x}, 0) \in \tilde{\Omega}_\varepsilon$ with $|\bar{x}_i - \bar{x}_j|$ arbitrarily large.

5.2.2 Proof of Step 2

Since all agents are arbitrarily far one from each other, we have $F_i(x) \simeq 0$ for $i = 1, \dots, N$. We can now steer all agents to a circular equidistributed configuration of large radius R, again by quasi-static deformation, as follows. Choose a point x^* of the plane, that does not belong to any of the lines passing through $(\bar{x}_i, \bar{x}_j)$ and apply a coordinate translation to have $x^* = 0$. We want to steer each particle $x_i(t)$ starting at $\bar{x}_i$ along the half line starting at 0 and passing through $\bar{x}_i$, in order to reach the point $\tilde{x}_i$ with distance $R > \frac{\alpha}{\beta\varepsilon}$.The crucial observation is that each pairwise distance $|x_i(t) - x_j(t)|$ needs to be kept sufficiently large to ensure that $F_i \simeq 0$ along the motion. We denote by $L = \min_{i\neq j} |\bar{x}_i - \bar{x}_j|$ such a minimal distance.

Note that each angle $\widehat{\bar{x}_i x^* \bar{x}_j}$ is nonzero for $i \neq j$ by the choice of $x^* = 0$, hence there exists a minimal angle $\theta > 0$. Consider now one of the indices i realizing the maximal distance $|\bar{x}_i|$ (that we assume to be the index 1) and move it along the quasi-static trajectory $x_1(\tau) = \bar{x}_1 + \tau(\tilde{x}_1 - \bar{x}_1)$. Since $\bar{x}_1$ was chosen to realize the maximal distance, for each $j \neq 1$ the triangle with vertices $0, \bar{x}_j, x_1(\tau)$ has an internal angle α_j in $\bar{x}_j$ that is increasing with respect to time, hence the distance $|\bar{x}_j - x_1(\tau)|$ is increasing too (see Figure 7, left).

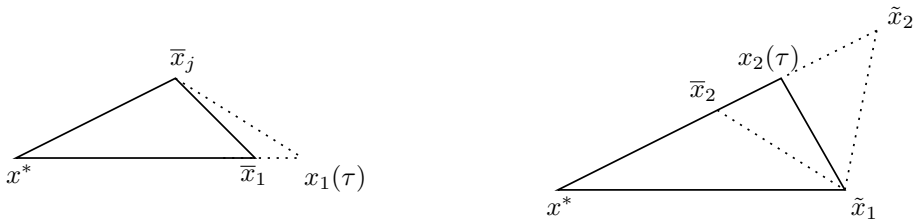

Figure 7: Left: Moving $x_1(\tau)$ increases the distance. Right: the minimum distance when moving $x_2(\tau)$ is realized by the right triangle.

We now choose one of the indices $i = 2, \dots N$ realizing the maximal distance $|x^* - \bar{x}_i|$, that we assume to be the index 2, and move it along the quasi-static trajectory $x_2(\tau) = x^* + \bar{x}_2 + \tau(\tilde{x}_2 - \bar{x}_2)$. It is then clear that the distance $|\bar{x}_j - x_2(\tau)|$ is increasing for all $j = 3, \dots N$, due to the same observation as above. Instead, the distance $|\tilde{x}_1 - x_2(\tau)|$ can eventually decrease, up to the minimum that is realized when the triangle with vertices $x^*, x_2(\tau), \tilde{x}_1$ is right in $x_2(\tau)$, see Figure 7, right. Such a minimal distance is thus larger than $R\sin(\theta)$, where θ is the minimal angle given above. By choosing $R > L/\sin(\theta)$, we are ensured that the minimal distance is greater than L.

Repeat the same construction for the indices 3 to N and hence steer all agents to a circle of radius R. By contruction, the pairwise distance is larger than L. Rearrange indices on the circle to have $\tilde{x}_i = R(\cos(\alpha_i), \sin(\alpha_i))$ with $0 < \alpha_1 < \alpha_2 < \dots \leqslant \alpha_N \leqslant 2\pi$. Consider now

the target equidistributed configuration with radius R: we simultaneously steer each $\tilde{x}_i$ to $\hat{x}_i = R(\cos(\frac{2i\pi}{N}), \sin(\frac{2i\pi}{N}))$ by using again a quasi-static deformation along the path

$$x_i(\tau) = R(\cos((1-\tau)\alpha_i + \tau\tfrac{2i\pi}{N}), \sin((1-\tau)\alpha_i + \tau\tfrac{2i\pi}{N})).$$

It is easy to verify that the simultaneous displacement along the circle ensures that the minimal distance $|x_i(\tau) - x_j(\tau)|$ is realized either at the beginning or at the end of the deformation, hence in all cases $|x_i(\tau) - x_j(\tau)| > L$.

5.2.3 Proof of Step 3

At the end of Step 3, we have steered the system to a circular equidistributed configuration $(\hat{x}, 0)$ of large radius $R > \bar{R}$ in $\tilde{\Omega}_\varepsilon$. Since pairwise distances are arbitrarily large, we also have $(\hat{x}, 0) \in \Omega_{\varepsilon'}$ for an arbitrarily small $\varepsilon' > 0$, i.e., we can go back to the original system (1) with the potential W. Since the system (1) is locally controllable around $(\hat{x}, 0)$, we can control it to a desired configuration, as follows.

Reaching a flock ring We first steer the system to $(\hat{x}, \varepsilon\bar{v})$ with $\varepsilon > 0$ small and $\bar{v}$ the desired unitary velocity direction. We then let the system evolve by choosing $u_i = F_i$, which ensures that all velocities satisfy $v_i(t) = v_j(t)$, hence $x_i(t) - x_j(t)$ keeps being constant, hence $F_i \simeq 0$ along the motion. This also ensures that all velocities v_i converge to $\sqrt{\frac{\alpha}{\beta}}\bar{v}$, as in Step 3.1 in the proof of Theorem 1.

We next reduce the flock radius. Note that each flock ring of radius r can be realized as a trajectory of the system (1), provided that the control can be chosen as $u_i = F_i$. In the case of the flock ring, we have $|x_i(t) - x_j(t)| \geqslant |x_i(t) - x_{i+1}(t)| = 2\sin(\frac{\pi}{N})\bar{R}$ and thus

$$\|F_i\| \leqslant \sup_{r > 2\sin(\frac{\pi}{N})\bar{R}} |U'(r)|.$$

The condition $\|u_i\| > \sup_{r>2\sin(\frac{\pi}{N})\bar{R}} |U'(r)|$ ensures that each flock ring of radius $r \geqslant R$ can indeed be realized as a trajectory of the system. Hence, by a quasi-static deformation, we can steer the system from a flock of radius r_1 to a flock of radius r_2 whenever $r_1, r_2 \geqslant \bar{R}$.

Reaching a mill ring We first steer the system to $(\hat{x}_i, \hat{v}_i)$ with $\hat{v}_i = \varepsilon x_i^\perp$ for some small $\varepsilon > 0$, by local controllability around $(\hat{x}_i, 0) \in \Omega_\varepsilon$. We choose $u_i = F_i - \frac{|v_i|^2}{R}\frac{x_i}{|x_i|}$ to ensure that each agent undergoes the correct centripetal force and moves along the circle of radius R. Note that $\|u\| \leqslant \varepsilon + \frac{\alpha}{\beta R} \leqslant 2\varepsilon$ due to $R > \frac{\alpha}{\beta\varepsilon}$, hence the control is arbitrarily small, as in Step 3.3 in the proof of Theorem 1.

Similarly to the flock ring, we next reduce the radius to a chosen $r \geqslant \bar{R}$. Note that each mill ring with such a radius is a trajectory of (1), provided that $u_i = F_i - \frac{|v_i|^2}{r}\frac{x_i}{|x_i|}$. By symmetry of the configuration, both F_i and $-\frac{|v_i|^2}{r}\frac{x_i}{|x_i|}$ are radial forces. Hence

$$\|u_i\| \leqslant \|F_i\| + \frac{\alpha}{\beta r} \leqslant \sup_{r > 2\sin(\frac{\pi}{N})\bar{R}} |U'(r)| + \frac{\alpha}{\beta\bar{R}} \leqslant M,$$

which ensures that any mill of radius $r \geqslant \bar{R}$ can be reached. Using a quasi-static deformation, we can steer the system from any mill ring of radius r_1 to any mill ring of radius r_2, whenever $r_1, r_2 \geqslant \bar{R}$.

References

[1] G. Albi, D. Balagué, J. A. Carrillo, and J. von Brecht. Stability analysis of flock and mill rings for second order models in swarming. *SIAM J. Appl. Math.*, 74(3):794–818, 2014.

[2] G. Albi, M. Bongini, E. Cristiani, and D. Kalise. Invisible control of self-organizing agents leaving unknown environments. *SIAM J. Appl. Math.*, 76(4):1683–1710, 2016.

[3] G. Albi, Y.-P. Choi, M. Fornasier, and D. Kalise. Mean field control hierarchy. *Appl. Math. Optim.*, 76(1):93–135, 2017.

[4] G. Albi, M. Herty, D. Kalise, and C. Segala. Moment-driven predictive control of mean-field collective dynamics. *arXiv preprint arXiv:2101.01970*, 2021.

[5] G. Albi and D. Kalise. (Sub)optimal feedback control of mean field multi-population dynamics. *IFAC-PapersOnLine*, 51(3):86–91, 2018.

[6] G. Albi, L. Pareschi, and M. Zanella. Boltzmann-type control of opinion consensus through leaders. *Philos. Trans. R. Soc. Lond. Ser. A Math. Phys. Eng. Sci.*, 372(2028):20140138, 18, 2014.

[7] I. Aoki. A simulation study on the schooling mechanism in fish. *Bull. Japan Soc. Sci. Fish*, 48:1081–1088, 1982.

[8] R. Bailo, M. Bongini, J. A. Carrillo, and D. Kalise. Optimal consensus control of the cucker-smale model. *IFAC-PapersOnLine*, 51(13):1 – 6, 2018.

[9] D. Balagué, J. A. Carrillo, T. Laurent, and G. Raoul. Dimensionality of local minimizers of the interaction energy. *Arch. Ration. Mech. Anal.*, 209(3):1055–1088, 2013.

[10] D. Balagué, J. A. Carrillo, T. Laurent, and G. Raoul. Nonlocal interactions by repulsive-attractive potentials: radial ins/stability. *Phys. D*, 260:5–25, 2013.

[11] A. B. T. Barbaro, K. Taylor, P. F. Trethewey, L. Youseff, and B. Birnir. Discrete and continuous models of the dynamics of pelagic fish: application to the capelin. *Math. Comput. Simulation*, 79(12):3397–3414, 2009.

[12] A. L. Bertozzi, T. Kolokolnikov, H. Sun, D. Uminsky, and J. Von Brecht. Ring patterns and their bifurcations in a nonlocal model of biological swarms. *Comm. Math. Sci.*, 13(4), 2015.

[13] B. Birnir. An ODE model of the motion of pelagic fish. *J. Stat. Phys.*, 128:535–568, 2007.

[14] M. Bongini, M. Fornasier, and D. Kalise. (Un)conditional consensus emergence under perturbed and decentralized feedback controls. *Discrete Contin. Dyn. Syst.*, 35(9):4071–4094, 2015.

[15] A. Borzi and S. Wongkaew. Modeling and control through leadership of a refined flocking system. *Math. Models Methods Appl. Sci.*, 25(02):255–282, 2015.

[16] S. Camazine, J. Deneubourg, N. R. Franks, J. Sneyd, G. Theraulaz, and E. Bonabeau. *Self-Organization in Biological Systems*. Princeton University Press, Princeton, 2001.

[17] M. Caponigro, M. Fornasier, B. Piccoli, and E. Trélat. Sparse stabilization and optimal control of the Cucker-Smale model. *Math. Control Rel. Fields*, 3(4):447–466, 2013.

[18] M. Caponigro, M. Fornasier, B. Piccoli, and E. Trélat. Sparse stabilization and control of alignment models. *Math. Mod. Meth. Appl. Sci.*, 25(03):521–564, 2015.

[19] M. Caponigro, B. Piccoli, F. Rossi, and E. Trélat. Mean-field sparse Jurdjevic–Quinn control. *Math. Models Methods Appl. Sci.*, 27(07):1223–1253, 2017.

[20] M. Caponigro, B. Piccoli, F. Rossi, and E. Trélat. Sparse Jurdjevic-Quinn stabilization of dissipative systems. *Automatica J. IFAC*, 86:110–120, 2017.

[21] J. A. Carrillo, M. G. Delgadino, and A. Mellet. Regularity of local minimizers of the interaction energy via obstacle problems. *Comm. Math. Phys.*, 343(3):747–781, 2016.

[22] J. A. Carrillo, M. R. D'Orsogna, and V. Panferov. Double milling in self-propelled swarms from kinetic theory. *Kin. Rel. Mod.*, 2:363–378, 2009.

[23] J. A. Carrillo, M. Fornasier, J. Rosado, and G. Toscani. Asymptotic flocking dynamics for the kinetic Cucker-Smale model. *SIAM J. Math. Anal.*, 42(1):218–236, 2010.

[24] J. A. Carrillo, M. Fornasier, G. Toscani, and F. Vecil. Particle, kinetic, and hydrodynamic models of swarming. In *Mathematical modeling of collective behavior in socio-economic and life sciences*, Model. Simul. Sci. Eng. Technol., pages 297–336. Birkhäuser, 2010.

[25] J. A. Carrillo, Y. Huang, and S. Martin. Explicit flock solutions for Quasi-Morse potentials. *European J. Appl. Math.*, 25(5):553–578, 2014.

[26] J. A. Carrillo, Y. Huang, and S. Martin. Nonlinear stability of flock solutions in second-order swarming models. *Nonlinear Anal. Real World Appl.*, 17:332–343, 2014.

[27] Y.-P. Choi, D. Kalise, J. Peszek, and A. A. Peters. A collisionless singular Cucker–Smale model with decentralized formation control. *SIAM J. Appl. Dyn. Sys.*, 18(4):1954–1981, 2019.

[28] Y.-P. Choi, D. Kalise, and A. A. Peters. Collisionless and decentralized formation control for strings, 2021. arXiv:2102.13621.

[29] Y. Chuang, M. R. D'Orsogna, D. Marthaler, A. Bertozzi, and L. Chayes. State transitions and the continuum limit for interacting, self-propelled particles. *Phys. D*, 232:33–47, 2007.

[30] J.-M. Coron and E. Trélat. Global steady-state controllability of one-dimensional semilinear heat equations. *SIAM J. Control Optim.*, 43(2):549–569 (electronic), 2004.

[31] J.-M. Coron and E. Trélat. Global steady-state stabilization and controllability of 1D semilinear wave equations. *Commun. Contemp. Math.*, 8(4):535–567, 2006.

[32] F. Cucker and S. Smale. Emergent behavior in flocks. *IEEE Trans. Automat. Control*, 52(5):852–862, 2007.

[33] F. Cucker and S. Smale. On the mathematics of emergence. *Jpn. J. Math.*, 2(1):197–227, 2007.

[34] M. R. D'Orsogna, Y.-L. Chuang, A. L. Bertozzi, and L. S. Chayes. Self-propelled particles with soft-core interactions: patterns, stability, and collapse. *Physical review letters*, 96(10):104302, 2006.

[35] S.-Y. Ha and J.-G. Liu. A simple proof of the Cucker-Smale flocking dynamics and mean-field limit. *Commun. Math. Sci.*, 7(2):297–325, 2009.

[36] S.-Y. Ha and E. Tadmor. From particle to kinetic and hydrodynamic descriptions of flocking. *Kinet. Relat. Models*, 1(3):415–435, 2008.

[37] C. K. Hemelrijk and H. Hildenbrandt. Self-organized shape and frontal density of fish schools. *Ethology*, 114:245–254, 2008.

[38] M. Herty and D. Kalise. Suboptimal nonlinear feedback control laws for collective dynamics. In *Proceedings 2018 IEEE 14th ICCA*, pages 556–561, 2018.

[39] A. Huth and C. Wissel. The simulation of fish schools in comparison with experimental data. *Ecol. Model.*, 75/76:135–145, 1994.

[40] V. Jurdjevic and J. P. Quinn. Controllability and stability. *J. Differential Equations*, 28(3):381–389, 1978.

[41] H. K. Khalil. *Nonlinear systems; 3rd ed.* Prentice-Hall, 2002.

[42] D. Ko and E. Zuazua. Asymptotic behavior and control of a "guidance by repulsion" model. *Math. Models Methods Appl. Sci.*, 30(04):765–804, 2020.

[43] A. L. Koch and D. White. The social lifestyle of myxobacteria. *BioEssays*, 20(12):1030–1038, 1998.

[44] T. Kolokolnikov, J. A. Carrillo, A. Bertozzi, R. Fetecau, and M. Lewis. Emergent behaviour in multi-particle systems with non-local interactions [Editorial]. *Phys. D*, 260:1–4, 2013.

[45] T. Kolokonikov, H. Sun, D. Uminsky, and A. Bertozzi. Stability of ring patterns arising from 2d particle interactions. *Physical Review E*, 84(1):015203, 2011.

[46] E. B. Lee and L. Markus. *Foundations of optimal control theory.* John Wiley & Sons, Inc., New York-London-Sydney, 1967.

[47] H. Levine, W.-J. Rappel, and I. Cohen. Self-organization in systems of self-propelled particles. *Phys. Rev. E*, 63:017101, Dec 2000.

[48] R. Lukeman, Y. Li, and L. Edelstein-Keshet. Inferring individual rules from collective behavior. *Proc. Natl. Acad. Sci. U.S.A.*, 107(28):12576–12580, 2010.

[49] S. Motsch and E. Tadmor. Heterophilious dynamics enhances consensus. *SIAM Rev.*, 56(4):577–621, 2014.

[50] J. Parrish and L. Edelstein-Keshet. Complexity, pattern, and evolutionary trade-offs in animal aggregation. *Science*, 284(5411):99 –101, 1999.

[51] B. Piccoli, N. Pouradier Duteil, and E. Trélat. Sparse control of Hegselmann-Krause models: black hole and declustering. *SIAM J. Control Optim.*, 57(4):2628–2659, 2019.

[52] B. Piccoli and F. Rossi. Measure-theoretic models for crowd dynamics. In *Crowd Dynamics, Volume 1*, pages 137–165. Springer, 2018.

[53] B. Piccoli, F. Rossi, and E. Trélat. Control to flocking of the kinetic Cucker-Smale model. *SIAM J. Math. Anal.*, 47(6):4685–4719, 2015.

[54] C. Pouchol, E. Trélat, and E. Zuazua. Phase portrait control for 1D monostable and bistable reaction-diffusion equations. *Nonlinearity*, 32(3):884–909, 2019.

[55] E. D. Sontag. *Mathematical control theory*, volume 6. Springer, 2013.

[56] M. W. Spong, S. Hutchinson, and M. Vidyasagar. *Robot modeling and control*. John Wiley & Sons, 2nd edition, 2004.

[57] E. Trélat. *Contrôle optimal*. Mathématiques Concrètes. [Concrete Mathematics]. Vuibert, Paris, 2005. Théorie & applications. [Theory and applications].

[58] J. von Brecht, D. Uminsky, T. Kolokolnikov, and A. Bertozzi. Predicting pattern formation in particle interactions. *Math. Mod. Meth. Appl. Sci.*, 22:1140002, 2012.

[59] S. Wongkaew, M. Caponigro, and A. Borzi. On the control through leadership of the Hegselmann–Krause opinion formation model. *Math. Models Methods Appl. Sci.*, 25(03):565–585, 2015.